Rational Design, Synthesis, and X-ray Structure of Selective Noncovalent Thrombin Inhibitors

Jürgen Wagner,* Jörg Kallen, Claus Ehrhardt, Jean-Pierre Evenou, and Dieter Wagner

Novartis Pharma AG, CH-4002 Basel, Switzerland

Received March 17, 1998

We have designed, synthesized, and tested in vitro a novel class of noncovalent thrombin inhibitors. The main feature of these inhibitors is a 6,5-fused bicyclic core structure that fills the S_2 pocket of the active site of thrombin. The bicycle introduces conformational constraint into the ligand and locks the X_{aa}−Pro amide bond into the desired trans configuration. Among the known ring systems, we selected by molecular modeling the 7-thiaindolizidinones (BTD) as our basic template. The influence of several structural features was analyzed: the length of the argininal side chain, the stereochemistry at C_6, and the importance of making optimal use of the S_3 pocket. Finally, an X-ray crystal structure of inhibitor **15** bound to thrombin was obtained at a resolution of 2.3 Å. These designed thrombin inhibitors, which were prepared by an efficient synthesis, showed high selectivity over trypsin and other serine proteases. Further derivation based on the information obtained by X-ray crystallography should certainly allow to improve the potency.

Introduction

Thrombosis is a major cause of morbidity and mortality in the industrial world. The currently available drugs, heparins and coumarins, are unsatisfactory in many ways. For instance, both classes of compounds require careful monitoring of the patient to avoid serious bleeding. Therefore, new orally bioavailable antithrombotics are needed to replace those that are used nowadays.[1] One approach actively pursued is the development of a *direct* thrombin inhibitor. Thrombin is a trypsin-like serine protease with many functions.[2] Predominantly, it is the key terminal protease in the coagulation cascade and plays a central role in both hemostasis and thrombosis. Thrombin effectively catalyzes the proteolytic cleavage of the soluble plasma protein fibrinogen to form insoluble fibrin leading to clot formation. Considerable efforts have been devoted to the discovery of novel classes of inhibitors, which are safe, selective, and orally bioavailable and show a long duration of action.[3] Most inhibitors form a covalent bond with Ser 195 located in the active site of thrombin and are based on the initial observation that the chloromethyl ketone of D-Phe-Pro-Arg (PPACK) could mimic the sequence of fibrinogen. These inhibitors bear an electrophilic functionality like a boronic acid, an aldehyde, a ketoamide, or a fluoromethyl ketone. However, all these inhibitors possess a reactive functional group and therefore present several common problems, like lack of selectivity over other trypsin-like enzymes, rapid clearance, and low oral bioavailability. In this paper, we disclose a novel series of compounds, which belong to the noncovalent class of inhibitors. Their main feature is a 6,5-fused bicyclic ring system, which occupies the S_2 binding pocket in the active site of thrombin.

Design

Noncovalent thrombin inhibitors are molecules that do not interact covalently with Ser 195 but rather form strong hydrophobic and electrostatic interactions with the enzyme. A prominent example of this class of compounds is hirudin, a 65-aa peptide extracted from the leech *Hirudo medicinalis*.[4] Hirudin interacts with the enzyme in two ways. The N-terminus of hirudin binds to the enzyme active site with the polypeptide chain running in a direction opposite to that expected for a substrate, whereas the highly acidic C-terminal part binds to the negatively charged exosite of thrombin. The affinity of hirudin for thrombin is very high: $K_i = 10^{-14}$ M. Among the low-molecular-weight compounds, early prototypes of the noncovalent class of inhibitors, argatroban[5] and NAPAP,[6] were the result of careful structure−activity relationship (SAR) studies (Figure 1). Argatroban is a highly thrombin-selective inhibitor in development. This initial success as well as structural information from X-ray crystals of both NAPAP and argatroban[7] bound to human α-thrombin prompted the search for other nonelectrophilic thrombin inhibitors. The replacement of the basic guanidino moiety of argatroban has been an active field of research.[8] Along a similar line, CRC 220[9] and napsagatran[10] are two additional compounds showing very potent in vitro activity. The latter is extremely selective over trypsin but suffers from a lengthy synthesis. More recently, other inhibitors, possessing completely novel structures, were disclosed in the literature.[11] Among them, two ligands are particularly noteworthy: inogatran,[12] which is a very potent inhibitor based on a tripeptide motif, and the conformationally very rigid tricyclic inhibitor published by Obst et al.[13]

Except for the last example, all noncovalent thrombin inhibitors developed so far are highly flexible molecules. They can adopt multiple conformations due to numerous freely rotatable single bonds. On the other hand, it is a well-established principle that the affinity of a ligand will increase if its conformational flexibility in solution is limited to the bound conformation. Clearly, this

S0022-2623(98)01013-9 CCC: $15.00
Published on Web 08/25/1998

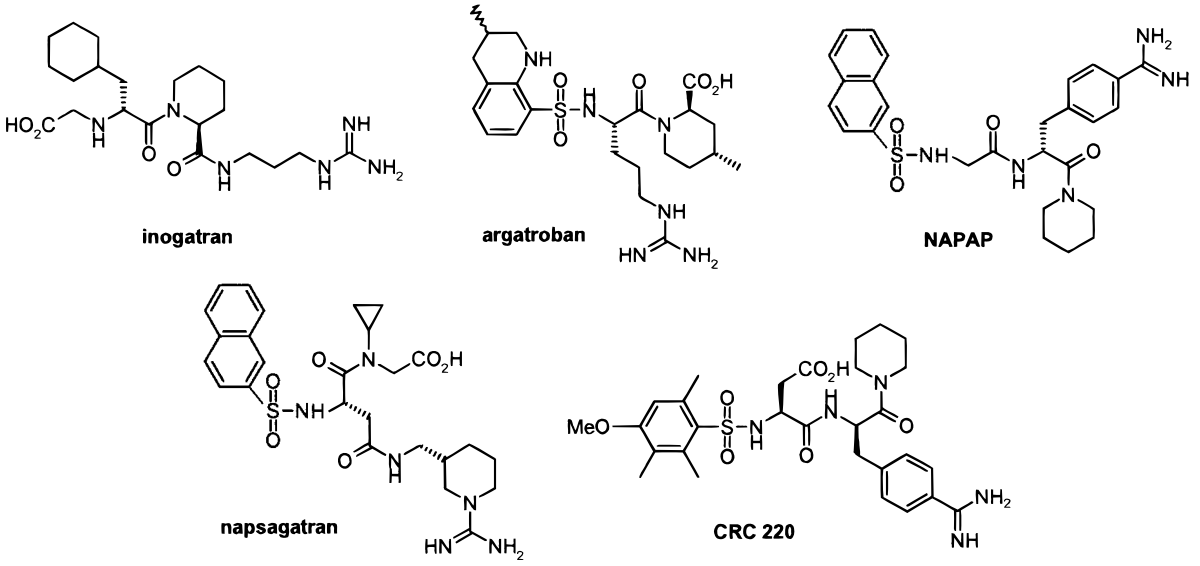

Figure 1. Selection of important noncovalent thrombin inhibitors.

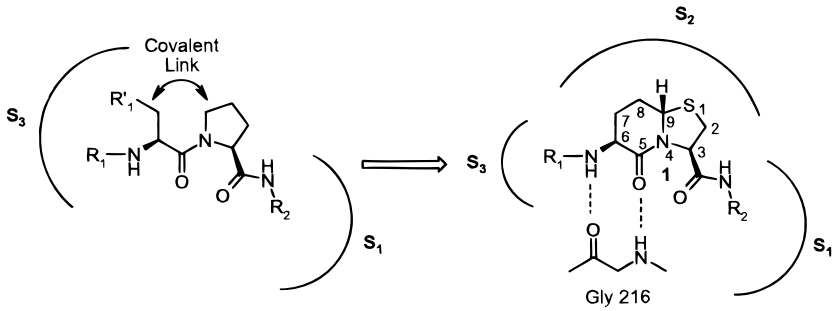

Figure 2. Addition of a covalent link between C_5 of proline and the adjacent amino acid locks the amide bond into the trans configuration. Structure of 7-thiaindolizidinone amino acid **1** (*S*-BTD).

statement proves true only if all hydrogen bonds and hydrophobic interactions between the ligand and the protein are maintained in the right position.[14] In the case of thrombin, the S_2 binding site is often occupied by proline or another *monocyclic* amino acid. We reasoned that the flexibility could be further reduced by replacing the *monocyclic* amino acid by a fused *bicyclic* system (Figure 2). The 6,5-bicyclic ring system, which should fill the S_2 binding site of the enzyme, can be viewed as the result of a covalent link between the C_5 position of proline and the adjacent amino acid. A definite advantage of such a template is that the X_{aa}−Pro amide bond is locked into the trans configuration, permitting the formation of two important hydrogen bonds with Gly 216 of thrombin as found in most potent inhibitors. In freely rotatable molecules, the cis isomer, which cannot bind to thrombin, might be present in considerable amounts (2−11%) under physiological conditions, because the difference in free energy between the cis and trans isomers of X_{aa}−Pro is small (0.5 kcal/mol).[15] In addition to having carbonyl and amine functionalities at C_5 and C_6, respectively, the ideal bicycle should fulfill several important criteria. Two attachment points are necessary: one at C_3 possessing the *S* configuration which will provide the attachment for the guanidino fragment and the second at C_6 for the attachment of a hydrophobic residue filling out the S_3 binding site. The "upper" surface of the bicycle, located below the flap formed by Trp 60D, should be hydrophobic. Finally, a short and stereoselective synthesis of the bicycle is desirable in order to have a practical approach to this novel class of ligands.

A search of the literature provided a number of fused bicyclic systems that were of interest. The 7-thiaindolizidinone amino acid **1** (Figure 2), which has been introduced by Nagai et al.,[16] was selected. It has first been used as a mimetic for a ***β*-t**urn **d**ipeptide and is therefore often abbreviated BTD. The thiaza[4.3.0]-alkane amino acid **1** is stable under physiological conditions and has been introduced into various peptides[17] and biologically active molecules.[18] The X-ray crystal structure of a derivative of BTD is available[19] and was used as a starting point for our molecular modeling studies (see the Experimental Section). The calculations indicated that BTD had the adequate structural characteristics to serve as a building block for thrombin inhibitors. Unfortunately the molecular modeling studies could not establish unambiguously the optimal configuration for binding at C_6. Therefore, we decided to synthesize and evaluate both bicycles in parallel.

Chemistry

The originally published 7-thiaindolizidinone (*S*-BTD) **1** possesses the *S* configuration at C_6 and can be prepared by various synthetic routes.[20] In our case, we also needed the *R*-BTD building block with the *R* configuration at C_6. The synthesis is outlined in Scheme 1 and was adapted from the original procedure for *S*-BTD.[16] Starting from D-glutamic acid 5-methyl ester,

Scheme 1[a]

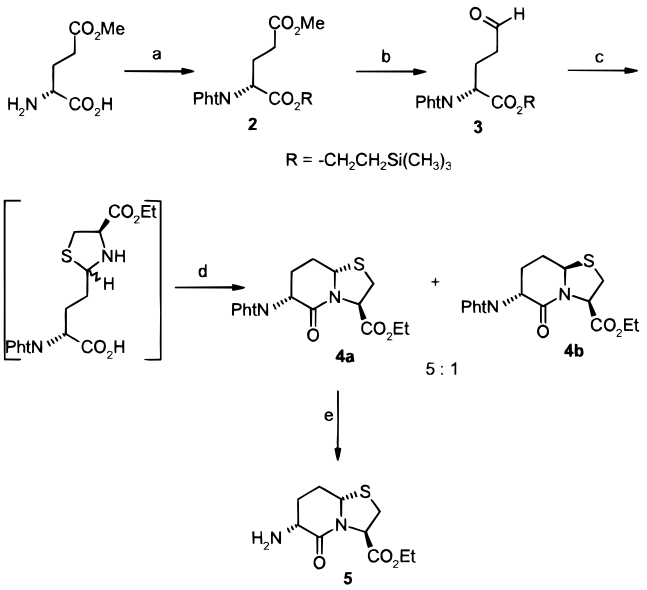

[a] (a) (i) *N*-(Ethoxycarbonyl)phthalimide, DMF, Et_3N, (ii) 2-(trimethylsilyl)ethanol, CH_2Cl_2, DMAP, DCC (73%); (b) DIBAL-H, Et_2O/CH_2Cl_2 (2:1), −78 °C (48%); (c) (i) L-Cys-OEt, EtOH/H_2O (10:1), NaOAc, AcOH, (ii) benzyltrimethylammonium fluoride, DMF; (d) CH_2Cl_2, 0.1 M HCl, (84% from **3**); (e) $NH_2NH_2 \cdot H_2O$, $CHCl_3$/EtOH (1:10) (61%).

the synthesis proceeded smoothly to the final acid-catalyzed cyclization (step d). The cyclization required an extended reaction time (4 days) and provided **4** as a 5:1 diastereomeric mixture at C_9. A similar isomeric ratio was noted by Schreiber et al.[17h] for a C_3,C_6-epimeric form of **4**. The isomers **4a**,**b** could be separated by preparative HPLC. ROESY ^1H NMR spectra provided clear evidence that the major diastereoisomer **4a** had the *S* and the minor **4b** the *R* configuration at C_9, respectively.[21] The phthalimido protecting group was removed by using hydrazine hydrate to afford the amine **5**.

The free amino functionality was then coupled to various sulfonyl chlorides or protected with the *tert*-butoxycarbonyl group (**6**−**8**) before the ethyl ester was hydrolyzed (Scheme 2). The free acid was coupled to Boc-protected alkylguanidines having two different chain lengths. Finally, all protecting groups were removed in one step to afford the inhibitors **13**−**16** as their trifluoroacetic acid salts.

In an analogous manner, the ligands **25**−**28** were obtained from Fmoc-protected *S*-BTD (Scheme 3). All the inhibitors were found to be very hygroscopic foams on which it was difficult to obtain suitable elemental analyses. Therefore, they were analyzed by reverse-phase HPLC (see the Experimental Section).

X-ray Crystallographic Structure of 15 Bound to Thrombin

To gain further insight into the ligand−protein interactions, the X-ray structure of **15** bound to human

Scheme 2[a]

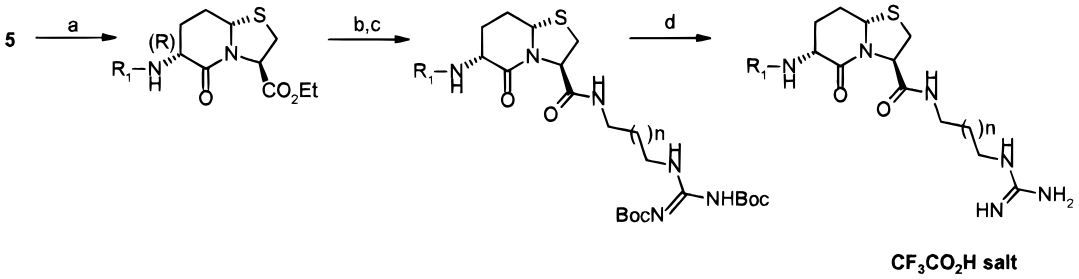

6: R_1 = Boc
7: R_1 = BenzylSO$_2$-
8: R_1 = 1-NaphthylSO$_2$-

9: n = 2; R_1 = Boc
10: n = 1; R_1 = Boc
11: n = 1; R_1 = BenzylSO$_2$-
12: n = 1; R_1 = 1-NaphthylSO$_2$-

13: n = 2; R_1 = H
14: n = 1; R_1 = H
15: n = 1; R_1 = BenzylSO$_2$-
16: n = 1; R_1 = 1-NaphthylSO$_2$-

[a] (a) $(Boc)_2O$, Et_3N, ^{t}BuOH or RSO_2Cl, Et_3N, CH_2Cl_2; (b) LiOH, MeOH/H_2O (5:1); (c) $H_2N(CH_2)_{3,4}NHC(=NBoc)NHBoc$ (**17** or **18**), EDCI, HOBT, CH_2Cl_2; (d) CH_2Cl_2/TFA (7:3).

Scheme 3[a]

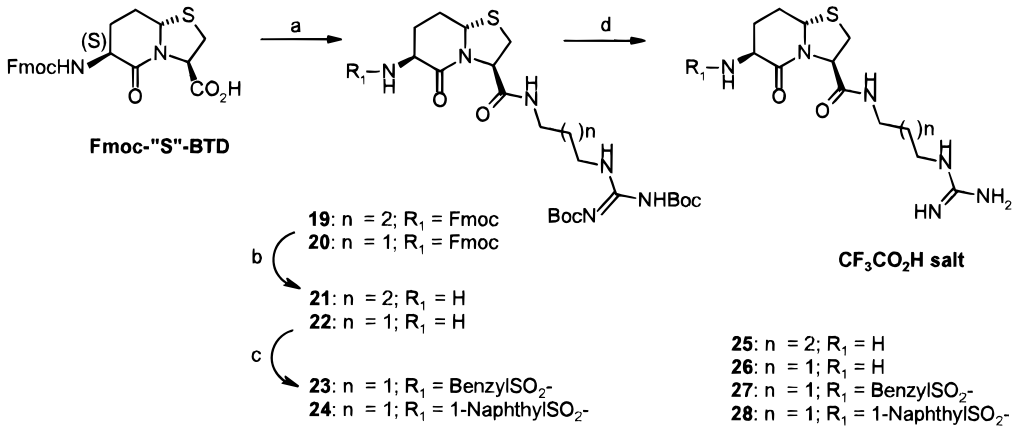

19: n = 2; R_1 = Fmoc
20: n = 1; R_1 = Fmoc

21: n = 2; R_1 = H
22: n = 1; R_1 = H

23: n = 1; R_1 = BenzylSO$_2$-
24: n = 1; R_1 = 1-NaphthylSO$_2$-

25: n = 2; R_1 = H
26: n = 1; R_1 = H
27: n = 1; R_1 = BenzylSO$_2$-
28: n = 1; R_1 = 1-NaphthylSO$_2$-

[a] (a) $H_2N(CH_2)_{3,4}NHC(=NBoc)NHBoc$ (**17** or **18**), EDCI, HOBT, CH_2Cl_2; (b) CH_2Cl_2/piperidine (8:2); (c) RSO_2Cl, Et_3N, CH_2Cl_2; (d) CH_2Cl_2/TFA (7:3).

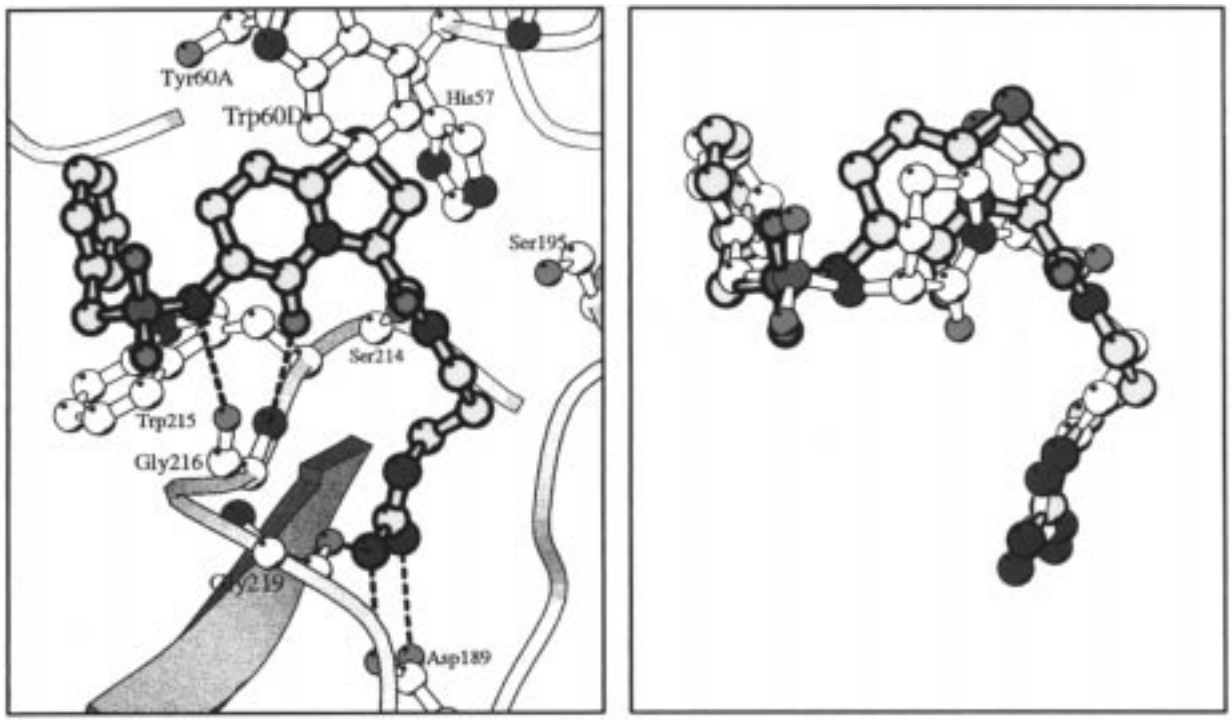

Figure 3. Left: Representation of the crystal structure of inhibitor **15** (yellow) bound to thrombin. Right: Superimposition, based on Cα's, of the X-ray crystal structure (yellow) and the results obtained by molecular modeling (white) for **15**.

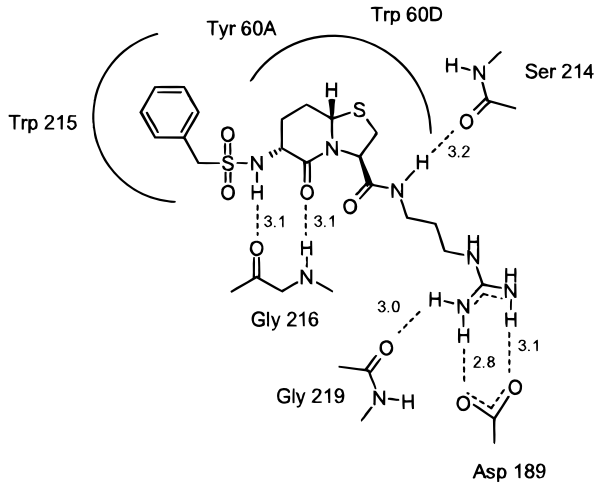

Figure 4. Schematic illustration of the key interactions of **15** with thrombin based on the crystal structure.

α-thrombin was determined. The resolution was 2.3 Å and the final *R*-factor 18.7% (for crystallographic details, see the Experimental Section). The X-ray crystal structure of thrombin-bound **15** confirmed partly the originally proposed binding mode (Figure 3, left). Compound **15** is bound to the active site of the enzyme with the argininal side chain extending into the S_1 pocket and making close electrostatic contacts with Asp 189 and Gly 219 (Figure 4). The benzyl group lies in the hydrophobic S_3 pocket interacting orthogonally with Trp 215. The 6,5-fused bicycle, *R*-BTD, fits nicely into the hydrophobic S_2 pocket. The bulky hydrophobic sulfur atom lies well-buried under the Trp 60D flap, and as expected, the two hydrogen bonds with Gly 216 are conserved. Thus all important interactions commonly found in low-molecular-weight thrombin inhibitors are present at the active site. Figure 3, right shows a superimposition of thrombin-bound **15** based on the results obtained from the X-ray crystal structure and the molecular modeling calculations. A major difference is the position occupied by *R*-BTD. The shift of the bicycle does not affect the argininal side chain and the benzyl group, which are similarly located in the S_1 and S_3 pockets, respectively. Remarkably, the carbonyl and the amino group interacting with Gly 216 are also located in very close proximity in each binding mode, emphasizing the importance of these two hydrogen bonds. A direct overlay of the two "proline" rings of the 7-thiaindolizidinone (data not shown) shows that the conformation of the six-membered ring is different from the X-ray structure of *S*-BTD found in the Cambridge Structural Database.[19] This conformational modification explains the two different positions occupied by the bicycle in Figure 3, right. The new conformation clearly has a positive effect on binding by allowing a better fit of the 7-thiaindolizidinone bicycle into the S_2 pocket without affecting the other important ligand−enzyme interactions.

As with other force fields, the torsional angle of the sulfonamide is not treated correctly within CHARMM (see the Experimental Part). The situation could be improved by changing the standard atom type for the nitrogen from NT (tetrahedral nitrogen) to NP (nitrogen in an amide bond). Even so this modification is not optimal; the results were found to be in reasonable agreement with the experimental measurements.

Biological Results and Discussion

The in vitro data for the thrombin inhibitors are summarized in Table 1. Chromogenic assays were carried out with important serine proteases including thrombin, trypsin, factor Xa, and plasmin. Selectivity ratios of trypsin/thrombin are tabulated. All inhibitors were found to be inactive against plasmin.

Table 1. In Vitro K_i Values (μM) of Selected Inhibitors Against Thrombin, Trypsin, and Factor Xa[a]

compd	thrombin	trypsin	factor Xa	Try/Thr
13	62.4 ± 2.4	5.36 ± 0.28	inactive at 100 μM	0.08
14	10.3 ± 0.32	25.1 ± 1.6	inactive at 100 μM	2.4
15	0.145 ± 0.008	5.10 ± 0.37	26.0 ± 2.5	35.2
16	0.751 ± 0.095	3.40 ± 0.16	6.78 ± 0.43	4.5
25	19.5 ± 0.9	3.58 ± 0.23	inactive at 100 μM	0.18
26	5.10 ± 0.49	13.3 ± 0.4	>33.7	2.6
27	0.111 ± 0.006	7.90 ± 0.17	>33.7	71.2
28	1.45 ± 0.08	19.6 ± 0.5	17.8 ± 0.9	13.5

[a] Mean ± SD of triplicate measurements.

Four compounds (**13**, **14**, **25**, **26**) lack a hydrophobic group to fill the S_3 pocket. Therefore it is not surprising that their inhibitory activity is low, but they provide useful information concerning selectivity. Substrates **13** and **25**, which have a longer argininal side chain ($n = 2$), show some selectivity for trypsin, whereas **14** and **26** are thrombin-selective. Previously, molecular modeling calculations had predicted that the optimal side chain length would be $n = 1$ rather than $n = 2$. These arguments prompted us to focus on the guanylated propyl side chain only. In the next step, we prepared the sulfonamides bearing bulky hydrophobic groups. The naphthyl derivatives **16** and **28** were clearly too bulky to fit the S_3 pocket. On the other hand, it has been very gratifying to find out that the benzylsulfonamides **15** and **27** have an almost 2 orders of magnitude higher potency than **14** and **26**. This considerable gain in binding indicates the necessity of making optimal use of the hydrophobic interactions in the S_3 pocket. The comparison of the *S*-BTD with the *R*-BTD series, which have the opposite stereochemistry at C_6, gave interesting results. Among all the inhibitors tested, the stereochemistry at C_6 had virtually no effect on the binding affinity: the *S*-BTD series being more potent by a factor of 3 at the most. The most potent inhibitor **27** had also a very good 70-fold selectivity over trypsin.

In conclusion, careful design using molecular modeling allowed us to develop very rapidly a novel class of direct noncovalent thrombin inhibitors with affinities in the nanomolar range. Their main characteristic is a fused 6,5-bicycle, which reduces the flexibility of the ligand. X-ray crystallography showed that inhibitor **15** satisfies all important ligand−protein interactions. On the other hand, it was found that the conformation of the 7-thiaindolizidinone bicycle (*R*-BTD) bound to thrombin was different form the published structure of *S*-BTD alone. The influence of the stereochemistry at C_6 on the potency of the inhibitors was found to be surprisingly low. Ligands with higher affinity should be obtained by further optimizing the fit of the ligand in the S_3 pocket.

Experimental Section

Chemistry. IR spectra were recorded on a Bruker IFS66 FT-IR spectrometer. FAB-MS and ESI-MS were measured on a VG 70SE and a Finnigan SSQ 7000 instrument, respectively. ^{1}H NMR spectra were determined on a Bruker AM spectrometer (360 MHz). Residual solvent peaks were employed as the internal reference ($CDCl_3$ 7.27 δ; DMSO 2.50 δ). Multiplicity is indicated by one or more of the following: s (singlet), d (doublet), t (triplet), q (quartet), m (multiplet), br (broad).

All reactions were monitored by TLC carried out on glass plates precoated (0.25 mm) with silica gel 60 F_{254}. Materials were detected by visualization under a UV lamp (254 nm) and/or using molybdenum solution followed by heat as developing agent. Flash column chromatography (FCC) was performed with Merck silica gel 60 (230−400 mesh). All mixed solvent systems are reported as v/v solutions. All reagents were purchased at highest commercial quality and used without further purification.

Carbamic Acid, [(4-Aminobutyl)carbonimidoyl]bis-, Bis(1,1-dimethylethyl) Ester (17). *N*-(Z)-1,4-diaminobutane (504 mg, 2.3 mmol) was dissolved in THF/H_2O 9:1 (5 mL). *N*,*N*′-Bis(*tert*-butoxycarbonyl)-*S*-methylisothiourea[22] (658 mg, 2.3 mmol) was added, and the mixture was stirred at room temperature for 48 h. The solvent was evaporated, and the residue was taken up in AcOEt (40 mL), washed twice with H_2O (10 mL), and dried over Na_2SO_4. After evaporation of the solvent, the residue was purified by FCC (AcOEt/hexane, 3:7) to afford the fully protected guanidine (947 mg, 90%) as a colorless oil: ^{1}H NMR (DMSO) δ 1.40, 1.47 (2s, 18H, 2Boc), 1.38−1.51 (m, 4H, H3, H4), 3.02 (m, 2H, H2), 3.26 (m, 2H, H5), 5.00 (s, 2H, PhC*H*$_2$OCO−), 7.23 (t, 1H, J = 5.5 Hz, *H*-N6), 7.26−7.39 (m, 5H, Ar*H*), 8.27 (t, 1H, J = 5.5 Hz, −OCON*H*−), 11.48 (s, 1H, *H*-N8); IR (neat) λ_{max} 3336, 2979, 2935, 1721, 1641, 1416, 1368, 1332, 1135; FAB-MS 465 $(M + H)^+$, 265 $(M + 2H - 2Boc)^+$; $C_{23}H_{36}N_4O_6$.

The guanidine (3.78 g, 8.1 mmol) was dissolved in EtOH (200 mL), and 10% Pd/C (0.5 g, 0.47 mmol) was added. The mixture was stirred under H_2 overnight. The suspension was filtered through Celite, and the solvent was evaporated to afford **17** (2.59 g, 96%) as a colorless oil: ^{1}H NMR (DMSO) δ 1.39, 1.48 (2s, 18H, 2Boc), 1.35−1.54 (m, 4H, H3, H4), 2.55 (t, 2H, J = 6.5 Hz, H2), 3.26 (t, 2H, J = 6.5 Hz, H5); IR (neat) λ_{max} 3320, 2980, 2933, 1717, 1637, 1417, 1368, 1330, 1132; FAB-MS 331 $(M + H)^+$, 231 $(M + H - Boc)^+$; $C_{15}H_{30}N_4O_4$.

Carbamic Acid, [(3-Aminopropyl)carbonimidoyl]bis-, Bis(1,1-dimethylethyl) Ester, Monohydrochloride (18). The first step of the preparation of **18** is identical to the procedure used for **17**, except that *N*-(*Z*)-1,3-diaminopropane was used in place of *N*-(*Z*)-1,4-diaminobutane. The fully protected guanidine (10.8 g, 71%) was obtained as white crystals: ^{1}H NMR (DMSO) δ 1.38, 1.47 (2s, 18H, 2Boc), 1.62 (m, 2H, H3), 3.02 (m, 2H, H2), 3.30 (m, 2H, H5), 5.01 (s, 2H, PhC*H*$_2$OCO−), 7.26 (t, 1H, J = 6.0 Hz, *H*-N5), 7.27−7.38 (m, 5H, Ar*H*), 8.34 (t, 1H, J = 6.0 Hz, −OCON*H*−), 11.47 (s, 1H, *H*-N7); IR (neat) λ_{max} 3334, 2979, 2920, 1722, 1643, 1135; FAB-MS 451 $(M + H)^+$, 251 $(M + 2H - 2Boc)^+$; $C_{22}H_{34}N_4O_6$.

The guanidine (450 mg, 1.0 mmol) was dissolved in EtOH (50 mL). Pd/C (10%) (200 mg, 0.2 mmol) and 1 M aqueous HCl (1.1 mL) were added. The mixture was stirred under H_2 for 3 h. The suspension was filtered through Celite, and the solvent was evaporated. The residue was redissolved in AcOEt (70 mL) and washed with H_2O/saturated aqueous NH_4OH (1:1) (20 mL). The organic phase was dried over Na_2SO_4 and evaporated to afford **18** (296 mg, 93%) as a colorless oil:[23] ^{1}H NMR (DMSO) δ 1.45, 1.51 (2s, 18H, 2Boc), 1.72 (m, 2H, H3), 2.78 (t, 2H, J = 6.5 Hz, H2), 3.50 (m, 2H, H4), 8.42 (br s, 1H, *H*-N5), 11.48 (s, 1H, *H*-N7); IR (neat) λ_{max} 3337, 2978, 2933, 1719, 1639, 1156, 1133; FAB-MS 317 $(M + H)^+$; $C_{14}H_{28}N_4O_4$.

Pentanedioic Acid, 2-(1,3-Dihydro-1,3-dioxo-2*H*-isoindol-2-yl)-, 5-Methyl 1-[2-(Trimethylsilyl)ethyl] Ester, (*R*)-(9Cl) (2). D-H-Glu(OMe)-OH hydrochloride (35.6 g, 0.18 mol) was dissolved in DMF (180 mL). Et_3N (62.7 mL, 0.45 mol) and *N*-(ethoxycarbonyl)phthalimide (39.0 g, 0.18 mol) were added, and the mixture was stirred for 16 h. The solvent was evaporated in vacuo, and the residue was redissolved in AcOEt (2 L). The organic phase was washed with 1 M aqueous HCl (3 × 400 mL) and brine (300 mL) and dried over Na_2SO_4. The solvent was evaporated to afford crude D-*N*-phthalimido-Glu-(OMe)-OH (∼55 g). The crude acid was dissolved in CH_2Cl_2 (600 mL) and cooled to 0 °C. This solution was treated sequentially with 2-(trimethylsilyl)ethanol (30 mL, 0.21 mol), DMAP (600 mg, 4.9 mmol), and DCC (40.2 g, 0.2 mol). The reaction was stirred for 15 h at room temperature, and the insoluble urea was removed by filtration. The solvent was evaporated, and the residue was purified by FCC (AcOEt/

hexane, 1:1) to afford **2** (51.5 g, 73%) as a colorless oil: ^{1}H NMR ($CDCl_3$) δ 0.0 (s, 9H, $-Si(CH_3)_3$), 0.98 (m, 2H, $-CH_2Si(CH_3)_3$), 2.40 (m, 2H, H4), 2.44−2.70 (m, 2H, H3), 3.62 (s, 3H, $-CO_2CH_3$), 4.24 (m, 2H, $-CO_2CH_2-$), 4.90 (dd, 1H, J = 5.5, 10.8 Hz, H2), 7.74−7.78 (m, 2H, Ar*H*), 7.84−7.89 (m, 2H, Ar*H*); IR (neat) λ_{max} 2954, 1778, 1740, 1720, 1388, 860, 839, 721; CI-MS (CH_4) 392 $(M + H)^+$, 304, 246; $C_{19}H_{25}NO_6Si$.

2*H*-Isoindole-2-acetic Acid, 1,3-Dihydro-1,3-dioxo-α-(3-oxopropyl)-, 2-(Trimethylsilyl)ethyl Ester, (*R*)-(9Cl) (3). To a solution of **2** (10 g, 25.5 mmol) in Et_2O/CH_2Cl_2 (2:1) (120 mL) cooled to −78 °C was added dropwise a 20% solution of DIBAL-H in toluene (32 mL, 36.0 mmol). The mixture was stirred for 25 min at −78 °C and then warmed to −50 °C. The solution was cannulated into a stirred ice-cold solution of half-saturated sodium potassium tartrate (240 mL). Et_2O (300 mL) was added, and the biphasic mixture was stirred for 3 h at room temperature. The phases were separated, and the aqueous phase was reextracted with AcOEt (150 mL). The combined organic phases were dried over Na_2SO_4 and evaporated. The residue was purified by FCC (AcOEt/hexane, 1:4) to afford **3** (4.4 g, 48%) as a colorless oil: ^{1}H NMR (DMSO) δ −0.5 (s, 9H, $-Si(CH_3)_3$), 0.87 (m, 2H, $-CH_2Si(CH_3)_3$), 2.15−2.29 (m, 1H, H3), 2.32−2.43 (m, 1H, H3), 2.56 (m, 2H, H4), 4.08−4.24 (m, 2H, $-CO_2CH_2-$), 4.86 (dd, 1H, J = 5.0, 10.5 Hz, H2), 7.83−7.95 (m, 4H, Ar*H*), 9.60 (s, 1H, −CO*H*); IR (neat) λ_{max} 2954, 1777, 1718, 1388, 1251, 860, 839, 722; FAB-MS 362 $(M + H)^+$, 288, 216; $C_{18}H_{23}NO_5Si$.

5*H*-Thiazolo[3,2-*a*]pyridine-3-carboxylic Acid, 6-(1,3-Dihydro-1,3-dioxo-2*H*-isoindol-2-yl)-hexahydro-5-oxo-, Ethyl Ester, [3*R*-(3α,6*β*,8aα)]-(9Cl) (4a) and 5*H*- Thiazolo-[3,2-*a*]pyridine-3-carboxylic Acid, 6-(1,3-Dihydro-1,3-dioxo-2*H*-isoindol-2-yl)-hexahydro-5-oxo-, Ethyl Ester, [3*R*-(3α,6*β*,8a*β*)]-(9Cl) (4b). To a stirred solution of the aldehyde **3** (4.4 g, 12.2 mmol) and sodium acetate (2.0 g, 24.4 mmol) in EtOH/H_2O 10:1 was added acetic acid (750 μL, 13.0 mmol) followed by L-H-Cys-OEt hydrochloride (2.4 g, 12.9 mmol). The solution was stirred for 17 h at room temperature, and the solvents were evaporated. The residue was taken up in CH_2Cl_2 (200 mL) and washed with 1 M aqueous HCl (200 mL). The aqueous phase was reextracted twice with CH_2Cl_2 (100 mL), and the combined organic phases were dried over Na_2SO_4 and evaporated. The crude product, a 1:1 mixture of diastereoisomers, was dissolved in DMF (80 mL) and treated with benzyltrimethylammonium fluoride (3.8 g, 20.3 mmol). The solution was stirred for 4 h at room temperature and then concentrated. The residue was taken up in CH_2Cl_2 (120 mL) and 1 M aqueous HCl (120 mL). The biphasic system was stirred vigorously for 4 days. The phases were separated, and the aqueous phase was extracted with CH_2Cl_2 (100 mL). The combined organic phases were dried over Na_2SO_4 and concentrated. The residue was purified by FCC (AcOEt/hexane, 4:1) to afford **4** (3.85 g, 84%) as a foam. The 5:1 diastereomeric mixture could be separated by reverse-phase preparative HPLC [C18, 25-min linear gradient; elution 30−100% H_2O/CH_3CN (1:9) in H_2O/CH_3CN (9:1); flow rate 20 mL/min]. **4a**: ^{1}H NMR (C_6D_6) δ 0.96 (t, 3H, J = 7.2 Hz, $-CO_2CH_2CH_3$), 1.51−1.66 (m, 2H, H7, H8), 2.00−2.11 (m, 1H, H8), 2.28−2.39 (m, 1H, H7), 2.96 (dd, 1H, J = 7.5, 10.5 Hz, H2), 3.02 (dd, 1H, J = 5.0, 10.5 Hz, H2), 3.95 (q, 2H, J = 7.2 Hz, $-CO_2CH_2CH_3$), 4.88 (dd, 1H, J = 4.7, 7.1 Hz, H9), 5.03 (dd, 1H, J = 7.3, 7.5 Hz, H6), 5.65 (dd, 1H, J = 5.0, 7.5 Hz, H3), 6.90−6.98 (m, 2H, Ar*H*), 7.48−7.55 (m, 2H, Ar*H*). **4b** ^{1}H NMR (C_6D_6) δ 1.02 (t, 3H, J = 7.1 Hz, −CO2CH2CH3), 1.67−1.78 (m, 2H, H7, H8), 1.78−1.90 (m, 1H, H8), 2.22−2.34 (m, 1H, H7), 2.64 (dd, 1H, J = 7.5, 12.5 Hz, H2), 2.75 (d, 1H, J = 12.5 Hz, H2), 4.02 (q, 2H, J = 7.1 Hz, $-CO_2CH_2CH_3$), 4.67 (dd, 1H, J = 2.8, 10.9 Hz, H9), 4.80 (d, 1H, J = 7.5 Hz, H3), 5.18 (dd, 1H, J = 6.4, 11.9 Hz, H6), 6.88−6.95 (m, 2H, Ar*H*), 7.49−7.55 (m, 2H, Ar*H*); IR (KBr) λ_{max} 2938, 1716, 1665, 1390, 1189, 719; FAB-MS 375 $(M + H)^+$, 301. $C_{18}H_{18}N_2O_5S$.[24]

5*H*-Thiazolo[3,2-*a*]pyridine-3-carboxylic Acid, 6-Amino-hexahydro-5-oxo-, Ethyl Ester, [3*R*-(3α,6*β*,8aα)]-(9Cl) (5). To a solution of **4a** (3.85 g, 10.3 mmol) in $CHCl_3$/EtOH (1:10) was added hydrazine monohydrate (2.25 mL, 46.4 mmol). The mixture was stirred for 48 h at room temperature. The solvent was evaporated and the residue redissolved in AcOEt (100 mL). The organic phase was washed with 0.2 M aqueous Na_2CO_3 (50 mL), dried over Na_2SO_4, and concentrated to afford **5** (1.53 g, 61%) as a yellowish oil: ^{1}H NMR ($CDCl_3$) δ 1.27 (t, 3H, J = 7.3 Hz, $-CO_2CH_2CH_3$), 1.75−2.45 (m, 4H, H7, H8), 3.16 (dd, 1H, J = 5.5, 11.5 Hz, H2), 3.20 (dd, 1H, J = 7.8, 11.5 Hz, H2), 3.52 (m, 1H, H6), 4.20 (q, 2H, J = 7.3 Hz, $-CO_2CH_2CH_3$), 4.92 (dd, 1H, J = 5.5, 7.0 Hz, H9), 5.28 (dd, 1H, J = 5.3, 7.8 Hz, H3); IR (neat) λ_{max} 3307, 2936, 1743, 1658, 1421, 1186; FAB-MS 245 $(M + H)^+$; $C_{10}H_{16}N_2O_3S$.

5*H*-Thiazolo[3,2-*a*]pyridine-3-carboxylic Acid, 6-[[(1,1-Dimethylethoxy)carbonyl]amino]-hexahydro-5-oxo-, Ethyl Ester, [3*R*-(3α,6*β*,8aα)]-(9Cl) (6). To a solution of **5** (300 mg, 1.2 mmol) and Et_3N (510 μL, 3.7 mmol) in ^{t}BuOH (20 mL) was added di-*tert*-butyl dicarbonate (800 mg, 3.7 mmol). The mixture was stirred overnight at room temperature and concentrated. The residue was redissolved in CH_2Cl_2 (50 mL) and washed with 1 M aqueous HCl (15 mL). The organic phase was dried over Na_2SO_4 and concentrated to afford **6** (410 mg, 97%) as a colorless oil: ^{1}H NMR ($CDCl_3$) δ 1.29 (t, 3H, J = 7.2 Hz, $-CO_2CH_2CH_3$), 1.45 (s, 9H, Boc), 1.63−2.10 (m, 2H, H7, H8), 2.20−2.52 (m, 2H, H7, H8), 3.22 (dd, 1H, J = 4.8, 11.5 Hz, H2), 3.30 (dd, 1H, J = 7.8, 11.5 Hz, H2), 4.10−4.30 (m, 3H, $-CO_2CH_2CH_3$, H6), 4.95 (dd, 1H, J = 5.5, 6.0 Hz, H9), 5.35 (dd, 1H, J = 4.8, 7.3 Hz, H3), 5.48 (br s, 1H, −OCON*H*−); IR (neat) λ_{max} 3366, 2977, 1717, 1669, 1169; FAB-MS 345 $(M + H)^+$, 289 $(M + H - C_4H_8)^+$, 245 $(M + H - Boc)^+$; $C_{15}H_{24}N_2O_5S$.

5*H*-Thiazolo[3,2-*a*]pyridine-3-carboxamide, *N*-[4-[[Bis-[[(1,1-dimethylethoxy)carbonyl]amino]methylene]amino]-butyl]-6-[[(1,1-dimethylethoxy)carbonyl]amino]-hexahydro-5-oxo-, [3*R*-(3α,6*β*,8aα)]-(9Cl) (9). **6** (140 mg, 0.41 mmol) was dissolved in MeOH/H_2O (5:1) (20 mL) and cooled to 0 °C. LiOH (70 mg, 2.9 mmol) was added, and the mixture was stirred at room temperature for 3 h. MeOH was partially evaporated, and CH_2Cl_2 (25 mL) was added. The organic phase was washed with H_2O (10 mL), dried over Na_2SO_4, and concentrated to afford the crude acid. To a solution of the acid in CH_2Cl_2 (15 mL) cooled to 0 °C were added sequentially EDCI (76.7 mg, 0.4 mmol), HOBT (54 mg, 0.4 mmol), and **17** (132 mg, 0.4 mmol) dissolved in CH_2Cl_2 (5 mL). The mixture was stirred overnight at room temperature and concentrated. The residue was purified by FCC (AcOEt/hexane, 4:1) to afford **9** (177 mg, 69%) as a white foam: ^{1}H NMR (DMSO) δ 1.39 (s, 18H, 2Boc), 1.48 (s, 9H, Boc), 1.35−1.50 (m, 4H, H13, H14), 1.68−1.72 (m, 1H, H7 or H8), 1.76−2.02 (m, 2H, H7 or H8), 2.14−2.25 (m, 1H, H7 or H8), 3.00−3.12 (m, 1H, H2), 3.17−3.32 (m, 5H, H2, H12, H15), 4.18 (m, 1H, H6), 4.87 (dd, 1H, J = 5.5, 6.0 Hz, H9), 4.97 (dd, 1H, J = 5.5, 7.0 Hz, H3), 7.04 (d, 1H, J = 7.2 Hz, −OCON*H*−), 8.00 (t, 1H, J = 5.5 Hz, *H*-N16), 8.25 (t, 1H, J = 5.5 Hz, *H*-N11), 11.48 (s, 1H, *H*-N18); IR (KBr) λ_{max} 3337, 2979, 2935, 1721, 1641, 1167, 1134, 1053; ESI-MS 651 $(M + Na)^+$, 629 $(M + H)^+$; $C_{28}H_{48}N_6O_8S$.

5*H*-Thiazolo[3,2-*a*]pyridine-3-carboxamide, 6-Amino-*N*-[4-[(aminoiminomethyl)amino]butyl]-hexahydro-5-oxo-, [3*R*-(3α,6*β*,8aα)]-(9Cl), Tri(trifluoroacetic acid) Salt (13). **9** (177 mg, 0.28 mmol) was dissolved in CH_2Cl_2 (20 mL) and cooled to 0 °C. Trifluoroacetic acid (9 mL) was added, and the mixture was stirred overnight at room temperature. The volatile material was evaporated to afford the trifluoroacetic acid salt of **13** (182 mg, 96%) as a white foam: ^{1}H NMR (DMSO) δ 1.36−1.51 (m, 4H, H13, H14), 1.80−1.92 (m, 1H, H7 or H8), 1.93−2.05 (m, 1H, H7 or H8), 2.13−2.36 (m, 2H, H7 or H8), 3.02−3.14 (m, 5H, H2, H12, H15), 3.34 (dd, 1H, J = 7.5, 12.0 Hz, H2), 4.02 (m, 1H, H6), 4.95 (dd, 1H, J = 5.5, 6.0 Hz, H9), 5.02 (dd, 1H, J = 5.5, 7.0 Hz, H3), 7.58 (br s, 1H, NH), 8.17 (br s, 1H, NH), 8.30 (br, 2H, NH); IR (neat) λ_{max} 3191 (br), 1659, 1182, 1134; ESI-MS 329 $(M + H)^+$; $C_{13}H_{24}N_6O_2S$. HPLC analysis [C18, isocratic; elution H_2O/CH_3CN (9:1) containing 0.1% TFA; flow rate 1.5 mL/min] indicated that the product was >98% pure.

5*H*-Thiazolo[3,2-*a*]pyridine-3-carboxamide, *N*-[3-[[Bis-[[(1,1-dimethylethoxy)carbonyl]amino]methylene]amino]-

propyl]-6-[[(1,1-dimethylethoxy)carbonyl]amino]-hexahydro-5-oxo-, [3*R*-(3α,6*β*,8aα)]-(9Cl) (10). This compound was prepared using the same procedure as described for **9**, except that the amine **17** was replaced by the amine **18**. **10** (208 mg, 74%) was obtained as a white foam: ^{1}H NMR ($CDCl_3$) δ 1.45 (s, 9H, Boc), 1.49, 1.51 (2s, 18H, 2Boc), 1.53−1.85 (m, 4H, H7, H8, H13), 2.27−2.43 (m, 2H, H7, H8), 3.18−3.22 (m, 4H, H2, H12, H14), 3.38−3.60 (m, 2H, H2, H12 or H14), 4.18 (m, 1H, H6), 5.00 (dd, 1H, J = 5.5, 6.0 Hz, H3 or H9), 5.08 (dd, 1H, J = 6.5, 7.0 Hz, H3 or H9), 5.47 (br, 1H, −OCON*H*−), 7.70 (br, 1H, *H*-N15), 8.46 (br, 1H, *H*-N11), 11.48 (s, 1H, *H*-N17); IR (KBr) λ_{max} 3335, 2979, 2935, 1722, 1642, 1167, 1135, 1051; ESI-MS 615 $(M + H)^+$; $C_{27}H_{46}N_6O_8S$.

5*H*-Thiazolo[3,2-*a*]pyridine-3-carboxamide, 6-Amino-*N*-[3-[(aminoiminomethyl)amino]propyl]-hexahydro-5-oxo-, [3*R*-(3α,6*β*,8aα)]-(9Cl), Tri(trifluoroacetic acid) Salt (14). This compound was prepared from **10** using the same procedure as described for **13**. The trifluoroacetic acid salt of **14** (198 mg, 89%) was obtained as a colorless oil: ^{1}H NMR (DMSO) δ 1.54−1.66 (m, 2H, H11), 1.67−2.05 (m, 2H, H7, H8), 2.12−2.36 (m, 2H, H7, H8), 2.98−3.17 (m, 5H, H2, H10, H12), 3.28−3.42 (m, 1H, H2), 3.93−4.05 (m, 1H, H6), 4.88−5.02 (m, 2H, H3, H9), 7.15 (br s, 3H, NH_3^+), 7.55 (s, 1H, NH), 8.20 (s, 1H, NH), 8.30 (br s, 2H, NH_2^+); IR (neat) λ_{max} 3192 (br), 1669, 1202, 1138; ESI-MS 315 $(M + H)^+$; $C_{12}H_{22}N_6O_2S$. HPLC analysis [C18, isocratic; elution H_2O/CH_3CN (9:1) containing 0.1% TFA; flow rate 1.5 mL/min] indicated that the product was >98% pure.

5*H*-Thiazolo[3,2-*a*]pyridine-3-carboxylic Acid, Hexahydro-5-oxo-6-[[(phenylmethyl)sulfonyl]amino]-, Ethyl Ester, [3*R*-(3α,6*β*,8aα)]-(9Cl) (7). To a solution of **5** (48 mg, 0.2 mmol) in CH_2Cl_2 (2 mL) cooled to 0 °C were added Et_3N (43 μL, 0.3 mmol) and benzenesulfonyl chloride (42 mg, 0.22 mmol). The mixture was stirred overnight at room temperature and concentrated. The residue was purified by FCC (AcOEt/hexane, 1:4, ∼200 mL; AcOEt/hexane, 1:1, ∼200 mL) to afford **7** (57 mg, 72%) as a colorless oil: ^{1}H NMR ($CDCl_3$) δ 1.31 (t, 3H, J = 7.2 Hz, $-CO_2CH_2CH_3$), 1.76−2.00 (m, 2H, H7, H8), 2.17−2.30 (m, 2H, H7, H8), 3.22 (dd, 1H, J = 5.5, 11.5 Hz, H2), 3.31 (dd, 1H, J = 7.2, 11.5 Hz, H2), 3.93 (m, 1H, H6), 4.25 (q, 2H, J = 7.2 Hz, $-CO_2CH_2CH_3$), 4.33 (d, 1H, J = 14.0 Hz, $-SO_2CH_2Ph$), 4.40 (d, 1H, J = 14.0 Hz, $-SO_2CH_2Ph$), 4.87 (dd, 1H, J = 5.5, 6.0 Hz, H9), 5.30 (m, 2H, H3, $-NHSO_2-$), 7.32−7.48 (m, 5H, Ar*H*); IR (neat) λ_{max} 3274, 2937, 1742, 1661, 1332, 1157, 1130, 699, 543; FAB-MS 399 $(M + H)^+$; $C_{17}H_{22}N_2O_5S_2$.

5*H*-Thiazolo[3,2-*a*]pyridine-3-carboxamide, *N*-[3-[[Bis-[[(1,1-dimethylethoxy)carbonyl]amino]methylene]amino]-propyl]-hexahydro-5-oxo-6-[[(phenylmethyl)sulfonyl]amino]-, [3*R*-(3α,6*β*,8aα)]-(9Cl) (11). To a solution of **7** (223 mg, 0.56 mmol) in MeOH/H_2O (5:1) (31 mL) was added LiOH (74 mg, 3.1 mmol). The mixture was stirred for 2 h at room temperature. MeOH was partially evaporated, and the residue was taken up in CH_2Cl_2 (20 mL). The organic phase was washed with 1 M aqueous HCl (10 mL) and H_2O (5 mL), dried over Na_2SO_4, and evaporated to afford the crude acid. To a solution of the acid in CH_2Cl_2 (32 mL) cooled to 0 °C were added EDCI (109 mg, 0.57 mmol) and HOBT (77 mg, 0.57 mmol). After 15 min, the amine **18** (245 mg, 0.77 mmol), dissolved in CH_2Cl_2 (16 mL), was added and the mixture was stirred for 1.5 h at 0 °C. The reaction was concentrated, and the residue was purified by FCC (AcOEt/hexane, 4:1) to afford **11** (260 mg, 69%) as a white foam: ^{1}H NMR ($CDCl_3$) δ 1.49 (s, 9H, Boc), 1.51 (s, 9H, Boc), 1.65−2.02 (m, 4H, H7, H8, H13), 2.15−2.30 (m, 2H, H7, H8), 3.22−3.39 (m, 4H, H2, H12, H14), 3.42−3.62 (m, 2H, H2, H14), 3.96 (m, 1H, H6), 4.33 (d, 1H, J = 13.5 Hz, $-SO_2CH_2Ph$), 4.38 (d, 1H, J = 13.5 Hz, $-SO_2CH_2Ph$), 4.96 (dd, 1H, J = 5.5, 6.0 Hz, H3 or H9), 5.04 (dd, 1H, J = 6.5, 7.0 Hz, H3 or H9), 5.32 (d, 1H, J = 5.0 Hz, $-SO_2NH-$), 7.32−7.48 (m, 5H, Ar*H*), 7.94 (br, 1H, *H*-N15), 8.48 (br, 1H, *H*-N11), 11.46 (s, 1H, *H*-N17); IR (KBr) λ_{max} 3330, 2979, 1723, 1643, 1330, 1134; FAB-MS 669 $(M + H)^+$, 469 $(M + 2H - 2Boc)^+$; $C_{29}H_{44}N_6O_8S_2$.

5*H*-Thiazolo[3,2-*a*]pyridine-3-carboxamide, *N*-[3-[(Aminoiminomethyl)amino]propyl]-hexahydro-5-oxo-6-[[(phenylmethyl)sulfonyl]amino]-, [3*R*-(3α,6*β*,8aα)]-(9Cl), Di(trifluoroacetic Acid) Salt (15). To a solution of **11** (260 mg, 0.39 mmol) in CH_2Cl_2 (35 mL) cooled to 0 °C was added trifluoroacetic acid (15 mL). The mixture was stirred overnight at room temperature and concentrated to afford the trifluoroacetic acid salt of **15** (240 mg, 76%) as a colorless oil: ^{1}H NMR (DMSO) δ 1.56−1.68 (m, 2H, H13), 1.75−2.24 (m, 4H, H7, H8), 3.04−3.16 (m, 6H, H2, H12, H14), 4.12 (m, 1H, H6), 4.39 (d, 1H, J = 13.5 Hz, $-SO_2CH_2Ph$), 4.46 (d, 1H, J = 13.5 Hz, $-SO_2CH_2Ph$), 4.87 (dd, 1H, J = 5.5, 6.5 Hz, H3 or H9), 4.96 (dd, 1H, J = 6.0, 6.5 Hz, H3 or H9), 7.31−7.44 (m, 5H, Ar*H*), 7.72 (d, 1H, J = 8.0 Hz, NH), 8.15 (br, 1H, NH); IR (neat) λ_{max} 3354 (br), 2940, 1664, 1202; FAB-MS 469 $(M + H)^+$; $C_{19}H_{28}N_6O_4S_2$. HPLC analysis [C18, 20-min linear gradient; elution 0−100% H_2O/CH_3CN (1:9) in H_2O/CH_3CN (9:1) both containing 0.1% TFA; flow rate 1.5 mL/min] indicated that the product was 95% pure.

5*H*-Thiazolo[3,2-*a*]pyridine-3-carboxylic Acid, Hexahydro-6-[[(1-naphthyl)sulfonyl]amino]-5-oxo-, Ethyl Ester, [3*R*-(3α,6*β*,8aα)]-(9Cl) (8). To a solution of **5** (98 mg, 0.4 mmol) in CH_2Cl_2 (4 mL) cooled to 0 °C were added Et_3N (85 μL, 0.6 mmol) and 1-naphthalenesulfonyl chloride (100 mg, 0.44 mmol). The mixture was stirred overnight at room temperature and concentrated. The residue was purified by FCC (AcOEt/hexane, 1:1) to afford **8** (113 mg, 65%) as a white foam: ^{1}H NMR ($CDCl_3$) δ 1.18 (t, 3H, J = 7.1 Hz, $-CO_2CH_2CH_3$), 1.81−2.09 (m, 2H, H7, H8), 2.10−2.40 (m, 2H, H7, H8), 3.13 (dd, 1H, J = 4.5, 11.7 Hz, H2), 3.27 (dd, 1H, J = 7.5, 11.7 Hz, H2), 3.75 (m, 1H, H6), 4.24 (q, 2H, J = 7.1 Hz, $-CO_2CH_2CH_3$), 4.85 (dd, 1H, J = 5.5, 6.0 Hz, H9), 5.25 (dd, 1H, J = 4.5, 7.5 Hz, H3), 6.09 (d, 1H, J = 2.5 Hz, $-SO_2NH-$), 7.48−7.78 (m, 3H, Ar*H*), 7.94 (d, 1H, J = 8.0 Hz, Ar*H*), 8.08 (d, 1H, J = 8.2 Hz, Ar*H*), 8.27 (d, 1H, J = 7.3 Hz, Ar*H*), 8.67 (d, 1H, J = 8.4 Hz, Ar*H*); IR (neat) λ_{max} 3268, 2980, 1742, 1663, 1331, 1164, 805, 773, 589; ESI-MS 498 $(M + CH_3CN)K^+$, 457 $(M + K)^+$, 435 $(M + H)^+$; $C_{20}H_{22}N_2O_5S_2$.

5*H*-Thiazolo[3,2-*a*]pyridine-3-carboxamide, *N*-[3-[[Bis-[[(1,1-dimethylethoxy)carbonyl]amino]methylene]amino]-propyl]-hexahydro-6-[[(1-naphthyl)sulfonyl)amino]-5-oxo-, [3*R*-(3α,6*β*,8aα)]-(9Cl) (12). This compound was prepared from **8** using the same procedure as described for **11**. **12** (148 mg, 88%) was obtained as a white foam: ^{1}H NMR ($CDCl_3$) δ 1.49 (s, 9H, Boc), 1.52 (s, 9H, Boc), 1.56 (m, 2H, H13), 1.85−2.04 (m, 2H, H7, H8), 2.13−2.37 (m, 2H, H7, H8), 3.07−3.42 (m, 6H, H2, H12, H14), 3.66 (m, 1H, H6), 4.92 (dd, 1H, J = 5.0, 6.0 Hz, H3 or H9), 4.96 (dd, 1H, J = 6.5, 7.0 Hz, H3 or H9), 6.15 (s, 1H, $-SO_2NH-$), 7.51−7.70 (m, 3H, Ar*H*), 7.78 (br, 1H, *H*-N15), 7.92 (d, 1H, J = 7.2 Hz, Ar*H*), 8.07 (d, 1H, J = 7.2 Hz, Ar*H*), 8.25 (d, 1H, J = 6.5 Hz, Ar*H*), 8.40 (br, 1H, *H*-N11), 8.65 (d, 1H, J = 7.2 Hz, Ar*H*), 11.45 (s, 1H, *H*-N17); IR (KBr) λ_{max} 3333, 2978, 2930, 1724, 1642, 1330, 1161, 1133, 772; FAB-MS 705 $(M + H)^+$, 505 $(M + 2H - 2Boc)^+$, 383; $C_{32}H_{44}N_6O_8S_2$.

5*H*-Thiazolo[3,2-*a*]pyridine-3-carboxamide, *N*-[3-[(Aminoiminomethyl)amino]propyl]-hexahydro-6-[[(1-naphthyl)sulfonyl]amino]-5-oxo-, [3*R*-(3α,6*β*,8aα)]-(9Cl), Di(trifluoroacetic acid) Salt (16). This compound was prepared from **12** using the same procedure as described for **15**. The trifluoroacetic acid salt of **16** (128 mg, 83%) was obtained as a white powder: ^{1}H NMR (DMSO) δ 1.52−1.70 (m, 3H, H13, H7 or H8), 1.78−1.89 (m, 2H, H7, H8), 2.03−2.13 (m, 1H, H7 or H8), 2.98−3.12 (m, 5H, H2, H12, H14), 3.25 (dd, 1H, J = 6.5, 11.5 Hz, H2), 4.03 (m, 1H, H6), 4.78 (dd, 1H, J = 6.0, 7.0 Hz, H3 or H9), 4.85 (dd, 1H, J = 6.0, 7.0 Hz, H3 or H9), 7.42 (br, 1H, *H*-N15), 7.58−7.73 (m, 3H, Ar*H*), 8.02 (br, 1H, *H*-N11), 8.06 (d, 1H, J = 7.2 Hz, Ar*H*), 8.20 (d, 1H, J = 7.2 Hz, Ar*H*), 8.28 (d, 1H, J = 7.2 Hz, Ar*H*), 8.50 (m, 1H, NH), 8.63 (d, 1H, J = 7.2 Hz, Ar*H*); IR (KBr) λ_{max} 3407, 2925, 1688, 1665, 1635, 1205, 1133, 804, 770, 596; ESI-MS 505 $(M + H)^+$; $C_{22}H_{28}N_6O_4S_2$. HPLC analysis [C18, 20-min linear gradient; elution 0−100%

H_2O/CH_3CN (1:9) in H_2O/CH_3CN (9:1) both containing 0.1% TFA; flow rate 1.5 mL/min] indicated that the product was 95% pure.

5*H*-Thiazolo[3,2-*a*]pyridine-3-carboxamide, *N*-[4-[[Bis-[[(1,1-dimethylethoxy)carbonyl]amino]methylene]amino]-butyl]-6-[[(9*H*-fluoren-9-ylmethoxy)carbonyl]amino]-hexahydro-5-oxo-, [3*R*-(3α,6*β*,8aα)]-(9Cl) (19). To a solution of Fmoc-BTD[20] (262 mg, 0.6 mmol) in CH_2Cl_2 (30 mL) cooled to 0 °C were added sequentially EDCI (153 mg, 0.8 mmol), HOBT (108 mg, 0.8 mmol), and the amine **17** (255 mg, 0.77 mmol) dissolved in CH_2Cl_2 (5 mL). The mixture was stirred overnight at room temperature and concentrated. The residue was purified by FCC (AcOEt/hexane, 1:1) to afford **19** (200 mg, 44%) as a white foam: ^{1}H NMR (DMSO) δ 1.38 (s, 9H, Boc), 1.46 (s, 9H, Boc), 1.35−1.45 (m, 4H, H13, H14), 1.72−2.05 (m, 3H, H7, H8), 2.27 (m, 1H, H7 or H8), 3.01−3.14 (m, 3H, H2, H12 or H15), 3.18−3.31 (m, 3H, H2, H12 or H15), 3.93 (m, 1H, H6), 4.23 (t, 1H, J = 6.0 Hz, −C*H*CH_2O−), 4.32 (d, 2H, J = 6.0 Hz, −CHC*H*$_2$O−), 4.85 (dd, 1H, J = 4.5, 10.5 Hz, H3 or H9), 4.97 (dd, 1H, J = 6.0, 7.0 Hz, H3 or H9), 7.32 (m, 2H, Ar*H*), 7.40 (m, 2H, Ar*H*), 7.68 (m, 3H, Ar*H*, NH), 7.88 (m, 3H, Ar*H*, NH), 8.23 (t, 1H, J = 6.0 Hz, *H*-N11), 11.47 (s, 1H, *H*-N18); IR (KBr) λ_{max} 3338, 2960, 1721, 1641, 1134, 741; ESI-MS 751 (M + H)$^+$; $C_{38}H_{50}N_6O_8S$.

5*H*-Thiazolo[3,2-*a*]pyridine-3-carboxamide, 6-Amino-*N*-[4-[[bis[[(1,1-dimethylethoxy)carbonyl]amino]methylene]amino]butyl]-hexahydro-5-oxo-, [3*R*-(3α,6α,8aα)]-(9Cl) (21). **19** (100 mg, 0.13 mmol) was dissolved in CH_2Cl_2/piperidine (8:2) and stirred for 30 min. The mixture was concentrated, and the residue was purified by FCC (AcOEt/EtOH/aqueous NH_3, 80:18:2) to afford **21** (48 mg, 68%) as a colorless oil: ^{1}H NMR (DMSO) δ 1.41 (s, 9H, Boc), 1.48 (s, 9H, Boc), 1.40−1.51 (m, 4H, H13, H14), 1.65−1.74 (m, 2H, H7, H8), 2.03−2.07 (m, 1H, H7 or H8), 2.25−2.31 (m, 1H, H7 or H8), 2.98 (dd, 1H, J = 6.0, 11.5 Hz, H2), 3.08 (m, 2H, H12 or H15), 3.23−3.34 (m, 4H, H2, H6, H12 or H15), 4.83 (dd, 1H, J = 6.0, 6.5 Hz, H3 or H9), 4.90 (dd, 1H, J = 5.5, 9.0 Hz, H3 or H9), 8.04 (t, 1H, J = 6.0 Hz, *H*-N16), 8.28 (t, 1H, J = 6.0 Hz, *H*-N11), 11.47 (s, 1H, *H*-N18); IR (KBr) λ_{max} 3337, 2935, 2979, 1722, 1641, 1134; ESI-MS 529 (M + H)$^+$; $C_{23}H_{40}N_6O_6S$.

5*H*-Thiazolo[3,2-*a*]pyridine-3-carboxamide, 6-Amino-*N*-[4-[(aminoiminomethyl)amino]butyl]-hexahydro-5-oxo-, [3*R*-(3α,6*β*,8aα)]-(9Cl), Tri(trifluoroacetic acid) Salt (25). This compound was prepared from **21** according to the same procedure as described for **13**. The trifluoroacetic acid salt of **25** (87 mg, 81%) was obtained as a white foam: ^{1}H NMR (DMSO) δ 1.38−1.51 (m, 4H, H13, H14), 1.78−2.00 (m, 2H, H7, H8), 2.15−2.25 (m, 1H, H7 or H8), 2.33−2.43 (m, 1H, H7 or H8), 2.97−3.18 (m, 6H, H2, H12, H15), 4.00 (m, 1H, H6), 4.85 (dd, 1H, J = 6.0, 7.0 Hz, H3 or H9), 4.92 (dd, 1H, J = 4.5, 11.0 Hz, H3 or H9), 7.58 (t, 1H, J = 5.5 Hz, *H*-N16), 8.18 (t, 1H, J = 5.5 Hz, *H*-N11), 8.35 (br, 3H, NH_3^+); IR (neat) λ_{max} 3200 (br), 1651, 1176, 1135; FAB-MS 329 (M + H)$^+$; $C_{13}H_{24}N_6O_2S$. HPLC analysis [C18, isocratic; elution H_2O/CH_3CN (9:1) containing 0.1% TFA; flow rate 1.5 mL/min] indicated that the product was >98% pure.

5*H*-Thiazolo[3,2-*a*]pyridine-3-carboxamide, *N*-[3-[[Bis-[[(1,1-dimethylethoxy)carbonyl]amino]methylene]amino]-propyl]-6-[[(9*H*-fluoren-9-ylmethoxy)carbonyl]-amino]-hexahydro-5-oxo-, [3*R*-(3α,6α,8aα)]-(9Cl) (20). This compound was prepared from Fmoc-BTD according to the same procedure as **19**, except that the amine **17** was replaced by the amine **18**. **20** (480 mg, 41%) was obtained as a white foam: ^{1}H NMR (DMSO) δ 1.40 (s, 9H, Boc), 1.46 (s, 9H, Boc), 1.58−1.68 (m, 2H, H13), 1.75−2.06 (m, 3H, H7, H8), 2.23−2.34 (m, 1H, H7 or H8), 3.03−3.15 (m, 3H, H2, H12 or H14), 3.27−3.38 (m, 3H, H2, H12 or H14), 3.96 (m, 1H, H6), 4.23 (t, 1H, J = 6.0 Hz, −C*H*CH_2O−), 4.33 (d, 2H, J = 6.0 Hz, −CHC*H*$_2$O−), 4.88−4.96 (m, 2H, H3, H9), 7.31 (m, 2H, Ar*H*), 7.42 (t, 2H, J = 6.5 Hz, Ar*H*), 7.70 (d, 2H, J = 6.5 Hz, Ar*H*), 7.78−7.86 (m, 2H, NH, *H*-N15), 7.90 (d, 2H, J = 6.5 Hz, Ar*H*), 8.35 (t, 1H, J = 6.0 Hz, *H*-N11), 11.47 (s, 1H, *H*-N17); IR (KBr) λ_{max} 3336, 2980, 1722, 1641, 1134, 741; ESI-MS 737 (M + H)$^+$; $C_{37}H_{48}N_6O_8S$.

5*H*-Thiazolo[3,2-*a*]pyridine-3-carboxamide, 6-Amino-*N*-[3-[[bis[[(1,1-dimethylethoxy)carbonyl]amino]methylene]amino]propyl]-hexahydro-5-oxo-, [3*R*-(3α,6α,8aα)]-(9Cl) (22). This compound was prepared from **20** according to the same procedure as **21**. **22** (385 mg, 98%) was obtained as a colorless oil: ^{1}H NMR (DMSO) δ 1.41 (s, 9H, Boc), 1.50 (s, 9H, Boc), 1.58−1.72 (m, 4H, H7, H8, H13), 2.02−2.10 (m, 1H, H7 or H8), 2.24−2.35 (m, 1H, H7 or H8), 2.98−3.15 (m, 3H, H2, H12 or H14), 3.18−3.25 (m, 1H, H6), 3.26−3.35 (m, 3H, H2, H12 or H14), 4.80 (dd, 1H, J = 6.5, 7.0 Hz, H3 or H9), 4.90 (dd, 1H, J = 5.5, 9.5 Hz, H3 or H9), 8.09 (t, 1H, J = 6.0 Hz, *H*-N15), 8.38 (t, 1H, J = 6.0 Hz, *H*-N11), 11.45 (s, 1H, *H*-N17); IR (neat) λ_{max} 3326, 2978, 1722, 1641, 1135, 735; ESI-MS 515 (M + H)$^+$; $C_{22}H_{38}N_6O_6S$.

5*H*-Thiazolo[3,2-*a*]pyridine-3-carboxamide, 6-Amino-*N*-[3-[(aminoiminomethyl)amino]propyl]-hexahydro-5-oxo-, [3*R*-(3α,6*β*,8aα)]-(9Cl), Tri(trifluoroacetic acid) Salt (26). This compound was prepared from **22** according to the same procedure as **25**. The trifluoroacetic acid salt of **26** (50 mg, 50%) was obtained as a colorless oil: ^{1}H NMR (DMSO) δ 1.56−1.68 (m, 2H, H13), 1.80−2.00 (m, 2H, H7, H8), 2.18−2.25 (m, 1H, H7 or H8), 2.35−2.44 (m, 1H, H7 or H8), 3.05 (dd, 1H, J = 6.0, 12.0 Hz, H2), 3.07−3.20 (m, 4H, H12, H14), 3.42 (dd, 1H, J = 9.5, 12.0 Hz, H2), 4.01 (m, 1H, H6), 4.83 (dd, 1H, J = 6.5, 7.0 Hz, H3 or H9), 4.94 (dd, 1H, J = 4.5, 11.5 Hz, H3 or H9), 7.15 (br, 3H, NH_3^+), 7.57 (t, 1H, J = 6.0 Hz, NH), 8.21 (t, 1H, J = 6.0 Hz, NH), 8.33 (br s, 3H, NH_3^+); IR (neat) λ_{max} 3192, 1668, 1202, 1137, 723; ESI-MS 315 (M + H)$^+$; $C_{12}H_{22}N_6O_2S$. HPLC analysis [C18, isocratic; elution H_2O/CH_3CN (9:1) containing 0.1% TFA; flow rate 1.5 mL/min] indicated that the product was >98%.

5*H*-Thiazolo[3,2-*a*]pyridine-3-carboxamide, *N*-[3-[[Bis-[[(1,1-dimethylethoxy)carbonyl]amino]methylene]amino]-propyl]-hexahydro-5-oxo-6-[[(phenylmethyl)sulfonyl]amino]-, [3*R*-(3α,6α,8aα)]-(9Cl) (23). To a solution of **22** (103 mg, 0.2 mmol) in CH_2Cl_2 (5 mL) cooled to 0 °C was added Et_3N (43 μL, 0.3 mmol) and benzenesulfonyl chloride (42 mg, 0.22 mmol). The mixture was stirred overnight at room temperature and concentrated. The residue was purified by FCC (AcOEt/EtOH/aqueous NH_3, 80:18:2) to afford **23** (71 mg, 53%) as a white foam: ^{1}H NMR (DMSO) δ 1.40 (s, 9H, Boc), 1.48 (s, 9H, Boc), 1.61−1.69 (m, 2H, H13), 1.78−1.99 (m, 2H, H7, H8), 2.05−2.15 (m, 1H, H7 or H8), 2.26−2.35 (m, 1H, H7 or H8), 3.03−3.16 (m, 4H, H2, H12, H14), 3.27−3.41 (m, 2H, H2, H12 or H14), 4.10 (m, 1H, H6), 4.49 (d, 1H, J = 13.5 Hz, −SO_2C*H*$_2$Ph), 4.55 (d, 1H, J = 13.5 Hz, −SO_2C*H*$_2$Ph), 4.87 (dd, 1H, J = 6.0, 6.5 Hz, H3 or H9), 4.92 (dd, 1H, J = 4.5, 10.5 Hz, H3 or H9), 7.28−7.44 (m, 5H, Ar*H*), 7.49 (d, 1H, J = 7.2 Hz, −SO_2N*H*−), 8.09 (t, 1H, J = 6.0 Hz, *H*-N15), 8.38 (t, 1H, J = 6.0 Hz, *H*-N11), 11.45 (s, 1H, *H*-N17); IR (KBr) λ_{max} 3331, 2978, 1723, 1642, 1329, 1134, 699; FAB-MS 669 (M + H)$^+$, 469 (M + 2H − 2Boc)$^+$; $C_{29}H_{44}N_6O_8S_2$.

5*H*-Thiazolo[3,2-*a*]pyridine-3-carboxamide, *N*-[3-[(Aminoiminomethyl)amino]propyl]-hexahydro-5-oxo-6-[[(phenylmethyl)sulfonyl]amino]-, [3*R*-(3α,6α,8aα)]-(9Cl), Di(trifluoroacetic acid) Salt (27). This compound was prepared from **23** according to the same procedure as **15**. The trifluoroacetic acid salt of **27** (30 mg, 82%) was obtained as a colorless oil: ^{1}H NMR (DMSO) δ 1.60−1.67 (m, 2H, H13), 1.79−1.98 (m, 2H, H7, H8), 2.08−2.16 (m, 1H, H7 or H8), 2.28−2.36 (m, 1H, H7 or H8), 3.05 (dd, 1H, J = 6.0, 12.0 Hz, H2), 3.08−3.18 (m, 4H, H12, H14), 3.39 (dd, 1H, J = 6.5, 12.0 Hz, H2), 4.10 (m, 1H, H6), 4.49 (d, 1H, J = 13.5 Hz, −SO_2C*H*$_2$-Ph), 4.54 (d, 1H, J = 13.5 Hz, −SO_2C*H*$_2$Ph), 4.86 (dd, 1H, J = 6.0, 6.5 Hz, H3 or H9), 4.92 (dd, 1H, J = 4.5, 11.0 Hz, H3 or H9), 7.25−7.47 (m, 5H, Ar*H*), 7.49 (d, 1H, J = 7.2 Hz, NH), 8.10 (t, 1H, J = 6.0 Hz, NH); IR (neat) λ_{max} 3351, 1668, 1203, 1131; FAB-MS 469 (M + H)$^+$; $C_{19}H_{28}N_6O_4S_2$. HPLC analysis [C18, 20-min linear gradient; elution 0−100% H_2O/CH_3CN (1:9) in H_2O/CH_3CN (9:1) both containing 0.1% TFA; flow rate 1.5 mL/min] indicated that the product was >98% pure.

**5*H*-Thiazolo[3,2-*a*]pyridine-3-carboxamide, *N*-[3-[[Bis-[[(1,1-dimethylethoxy)carbonyl]amino]methylene]amino]-propyl]-hexahydro-6-[[(1-naphthyl)sulfonyl]amino]-5-

oxo-, [3*R*-(3α,6α,8aα)]-(9Cl) (24). This compound was prepared from **22** according to the same procedure as **23**, except that benzenesulfonyl chloride was replaced by 1-naphthalenesulfonyl chloride. **24** (70 mg, 49%) was obtained as a white foam: ^{1}H NMR (DMSO) δ 1.40 (s, 9H, Boc), 1.49 (s, 9H, Boc), 1.54−1.64 (m, 2H, H13), 1.70−1.92 (m, 3H, H7, H8), 2.16−2.23 (m, 1H, H7 or H8), 2.96−3.04 (m, 2H, H2, H12 or H14), 3.07−3.17 (m, 1H, H12 or H14), 3.24−3.33 (m, 3H, H2, H12 or H14), 3.95 (m, 1H, H6), 4.76 (dd, 1H, J = 6.0, 6.5 Hz, H3 or H9), 4.88 (dd, 1H, J = 5.0, 10.5 Hz, H3 or H9), 7.58−7.72 (m, 3H, Ar*H*), 8.01 (t, 1H, J = 6.0 Hz, *H*-N15), 8.07 (d, 1H, J = 6.5 Hz, Ar*H*), 8.20 (d, J = 6.5 Hz, Ar*H*), 8.32 (t, 2H, J = 6.5 Hz, Ar*H*), 8.37 (t, 1H, J = 6.0 Hz, *H*-N11), 8.64 (d, 1H, J = 7.0 Hz, −SO_2N*H*−), 11.45 (s, 1H, *H*-N17); IR (KBr) λ_{max} 3329, 2977, 1723, 1641, 1134, 804, 772; FAB-MS 705 (M + H)$^+$, 505 (M + 2H − 2Boc)$^+$; $C_{32}H_{44}N_6O_8S_2$.

5*H*-Thiazolo[3,2-*a*]pyridine-3-carboxamide, *N*-[3-[(Aminoiminomethyl)amino]propyl]-hexahydro-6-[[(1-naphthyl)sulfonyl]amino]-5-oxo-, [3*R*-(3α,6α,8aα)]-(9Cl), Di(trifluoroacetic acid) Salt (28). This compound was prepared from **24** according to the same procedure as **15**. The trifluoroacetic acid salt of **28** (60 mg, 98%) was obtained as a white powder: ^{1}H NMR (DMSO) δ 1.56−1.65 (m, 2H, H13), 1.70−1.84 (m, 3H, H7, H8), 2.12−2.21 (m, 1H, H7 or H8), 2.97 (dd, 1H, J = 6.0, 12.0 Hz, H2), 3.05−3.16 (m, 4H, H12, H14), 3.30 (dd, 1H, J = 6.5, 12.0 Hz, H2), 3.96 (m, 1H, H6), 4.73 (dd, 1H, J = 6.0, 6.5 Hz, H3 or H9), 4.84 (dd, 1H, J = 5.0, 11.0 Hz, H3 or H9), 7.10 (br, 3H, NH_3^+), 7.40 (m, 1H, *H*-N11), 7.60−7.73 (m, 3H, Ar*H*), 8.03 (t, 1H, J = 6.0 Hz, NH), 8.09 (d, 1H, J = 7.0 Hz, Ar*H*), 8.22 (d, 1H, J = 7.0 Hz, Ar*H*), 8.26−8.35 (m, 2H, Ar*H*, NH), 8.63 (d, 1H, J = 7.0 Hz, Ar*H*); IR (KBr) λ_{max} 3366, 1663, 1203, 1161, 1131, 803, 592; ESI-MS 505 (M + H)$^+$; $C_{22}H_{28}N_6O_4S_2$. HPLC analysis [C18, 20-min linear gradient; elution 0−100% H_2O/CH_3CN (1:9) in H_2O/CH_3CN (9:1) both containing 0.1% TFA; flow rate 1.5 mL/min] indicated that the product was >98%.

Molecular Modeling. Molecular modeling started from the X-ray structure of the NAPAP/thrombin complex, structure 1DWD from the Brookhaven Protein Data Bank. The position of the Gly 216 carbonyl is unusual in this X-ray structure: the distance from the carbonyl oxygen to the NAPAP sulfonamide nitrogen is very short (2.27 Å), and the ψ angle is 156°. This angle is closer to 180° in other thrombin X-ray structures. The initial value of this angle was changed to −170° for this paper, and a harmonic constraint with a force constant of 10.0 was added to the carbonyl group of Gly 216. Test calculations showed that the carbonyl had a tendency to flip into a conformation with a ψ angle around 100° otherwise.

The X-ray structure of *S*-BTD was used for the bicyclic system.[19] The five-membered ring of the bicycle was manually docked into the S_2 binding site with the help of the in-house molecular graphics program WITNOTP. Further visual inspection showed that the optimal side chain attached at C_3 should have a length of three methylene units. This length would locate the guanidino group in an ideal position to form hydrogen bonds with Asp 189 in the S_1 pocket. The phenethyl and benzylsulfonyl moieties were attached at C_6 in the *R* and *S* configurations in order to evaluate the optimal space filling of the S_3 pocket. The starting structures were then minimized using CHARMM 23.[25] The atom types and charges were assigned within QUANTA 4.0.[25] The "charge templates" method was used with "charge smoothing" on carbons and nonpolar hydrogens to calculate the charges. All residues within 5 Å of the inhibitor were included into the minimization process, whereas the rest of the protein was kept fixed. Like other force fields, CHARMM does not calculate the dihedral angle of sulfonamides correctly. Due to a torsion potential with a periodicity of 3, conformations are generated in which the CN vector bisects the OSO angle in disagreement with experimental results. Test calculations with sulfonamides show that changing the atom type NT (tetrahedral nitrogen) automatically assigned by QUANTA into NP (nitrogen in an amide bond) improves the situation. However, optimal results for this torsion are obtained only if one reparametrizes this torsion using a different periodicity for the angle. The calculations showed that both residues were appropriate to fill the S_3 pocket. The *R* configuration looked somewhat better than the *S*; however, a clear preference could not be shown. As an example for the final minimized structures, the model of **15** complexed to thrombin is shown in Figure 3, right.

Table 2. Protein Crystallography Data Collection Statistics and Refinement Results

space group	*C*2
cell constants	
a (Å)	71.0
b (Å)	72.2
c (Å)	73.1
β (deg)	100.7
no. of complexes/asymmetric unit	1
data collection statistics	
resolution (Å)	15−2.3
no. of reflections measured	41060
no. of unique reflections	15423
R_{sym} (on intensities) overall	10.4
R_{sym} for 2.38−2.30 Å	43.2
% complete overall	95.0
% complete for 2.38−2.30 Å	94.6
number of refined non-H atoms	
protein	2615
inhibitor	31
solvent	200
R factor (no σ cutoff), before adding **15**	19.6
R factor (no σ cutoff)	18.7
R_{free} (a posteriori, 10% test set)	23.2
R factor for 2.4−2.3 Å	28.4
rms bond dev (Å)	0.015
rms angle dev (deg)	2.54
rms improper torsion dev (deg)	1.27
av *B* for protein (Å^2)	12.3
av *B* for inhibitor (Å^2)	22.4

Crystallography. Thrombin was prepared for crystallization according to a published procedure.[26] Crystals in the presence of benzamidine were grown at room temperature by seeding using the hanging-drop technique, similar to published procedures.[27] Typical reservoir conditions were 28% PEG8000, 50 mM NaPi, pH 7.3. Crystals grown in the presence of benzamidine were harvested into 0.1 mL of this buffer and soaked overnight in a 10 mM concentration of **15** (with two exchanges into fresh buffer). The binding of **15** to thrombin in the soaked crystal is complete as seen from the electron density and the crystals showing no cracking. The X-ray intensity data were collected on a FAST television area detector with an Enraf-Nonius FR571 rotating anode operating at 40 kV and 80 mA. Data were measured at room temperature in 160-s frames of width 0.2° in ω, a detector-swing-out angle of 20°, and a crystal-to-detector distance of 55 mm. The evaluation of the measured intensities was performed by the program MADNES.[28] Structure solution, refinement, and analysis were performed with the programs O[29] and X-PLOR.[30] Refinement was done using the target parameters of Engh and Huber.[31] Water molecules were added if found as a peak in the $F_o - F_c$ map (contoured at 3σ) making reasonable hydrogen bonds. Consult Table 2 for crystallographic details. The coordinates have been deposited at the Brookhaven Protein Data Bank under the PDB ID code 1bhx.

Chromogenic Assay. Human α-thrombin was purified in-house according to Stone et al.[32] Bovine pancreatic trypsin was purchased from Sigma. Human factor Xa was obtained from Boehringer Mannheim and human plasmin from KABI Vitrum. All Pefachrome substrates were purchased from Pentapharm, Basel, Switzerland.

Inhibitors were dissolved in cremophor/ethanol (1:1) and diluted in distilled water to yield a 1 mM solution. Further dilutions were made into assay buffer (100 mM sodium phosphate buffer, pH 7.4, containing 100 mM NaCl, and 0.1% bovine serum albumin). Kinetic assays were performed at 25 °C using a 96-microwell plate; each well contained 50 mL of substrate, 100 mL of inhibitor, and 100 mL of enzyme in assay

buffer. Final concentrations of enzyme and substrate were as follows: 160 pM α-thrombin and 100 mM Pefachrome TH (K_m = 7.5 mM), 260 pM trypsin and 500 mM Pefachrome TRY (K_m = 146 mM), and 30 pM FXa and 250 mM Pefachrome Xa (K_m = 127 mM). Assays were initiated by adding enzyme to solutions containing inhibitor and substrate. The release of *p*-nitroaniline by hydrolysis of the substrate was followed for 30 min by measuring the increase in optical density at 405 nm with a Thermomax microwell kinetic reader (Molecular Devices, Menlo Park, CA). The inhibition constant K_i was determined by fitting the data by weighted linear regression to the Dixon equation.[33] The dissociation constants were determined in triplicate and expressed as mean ± SD.

Acknowledgment. We are grateful to Dr. Mauro Zurini for the purification of human α-thrombin. We thank Bernhard Gafner for carrying out the biological assays and Armin Widmer for the use of WITNOTP.

References

(1) (a) Hirsh, J. Oral Anticoagulant Drugs. *New Engl. J. Med*. **1991**, *324*, 1865−1875. (b) New Antithrombotics: Better Agents are Needed to Prevent Blood Clots. *Genet. Technol. News* **1996**, *16*, 8 + 11. (c) Rihal, C. S.; Flather, M.; Hirsh, J.; Yusuf, S. Advances in Antithrombotic Drug Therapy for Coronary Artery Disease. *Eur. Heart J*. **1995**, *16*, 10−21.

(2) (a) Tapparelli, C.; Metternich, R.; Ehrhardt, C.; Cook, N. S. Synthetic Low-molecular Weight Thrombin Inhibitors: Molecular Design and Pharmacological Profile. *Trends Pharmacol. Sci.* **1993**, *14*, 366−376. (b) Bazan, J. F. Big Rigs in Blood Coagulation. *Nature* **1996**, *380*, 21−22. (c) Maraganore, J. M. Thrombin, Thrombin Inhibitors, and the Arterial Thrombotic Process. *Thromb. Haemostasis* **1993**, *70*, 208−211.

(3) (a) For an excellent review on the various classes of novel direct and indirect thrombin inhibitors, see: Balasubramanian, B. N., Ed. Advances in the Design and Development of Thrombin Inhibitors. *Bioorg. Med. Chem*. **1995**, *3*, 999−1156. (b) Kimball, S. D. Thrombin Active Site Inhibitors. *Curr. Pharm. Des.* **1995**, *1*, 441−468. (c) Edmunds, J. J.; Rapundalo, S. T.; Siddiqui, M. A. Thrombin and Factor Xa Inhibition. *Annu. Rep. Med. Chem*. **1996**, *31*, 51−60.

(4) (a) Lefkovits, J.; Topol, E. J. Direct Thrombin Inhibitors in Cardiovascular Medicine. *Circulation* **1994**, *90*, 1522−1536. (b) Tadeusz, P.; Cezary, W. Recombinant Hirudin. *Biotechnologia* **1996**, *3*, 34−42.

(5) (a) Kikumoto, R.; Tonomura, S.; Hara, H.; Ninomiya, K.; Maruyama, A.; Sugano, M.; Tamao, Y. Potent Inhibition of Thrombin by the Newly Synthesized Arginine Derivative No. 805. The Importance of Stereostructure of its Hydrophobic Carboxamide Portion. *Biochem. Biophys. Res. Commun*. **1981**, *101*, 440−446. (b) Okamoto, S.; Hijikata-Okunomiya, A. Synthetic Selective Inhibitors of Thrombin. *Methods Enzymol*. **1993**, *222*, 328−340.

(6) (a) Kaiser, B.; Hauptmann, J.; Weiss, A.; Markwardt, F. Pharmacological Characterization of a New Highly Effective Synthetic Thrombin Inhibitor. *Biomed. Biochim. Acta* **1985**, *44*, 1201−1210. (b) Kaiser, B.; Markwardt, F. Experimental Studies on the Antithrombotic Action of a Highly Effective Synthetic Thrombin Inhibitor. *Thromb. Haemostasis* **1986**, *55*, 194−196.

(7) (a) Turk, D.; Stürzebecher, J.; Bode, W. Geometry of Binding of the *N*α-Tosylated Piperidides of *m*-Amidino, *p*-Amidino- and *p*-Guanidino Phenylalanine to Thrombin and Trypsin. *FEBS* **1991**, *287*, 133−138. (b) Bode, W.; Turk, D.; Stürzebecher, J. Geometry of Binding of the Benzamidine- and Arginine-based Inhibitors N^{α}-(2-naphthyl-sulphonyl-glycyl)-DL-*p*-amidinophenylalanyl-piperidine (NAPAP) and (2*R*,4*R*)-4-methyl-1-[N^{α}-(3-methyl-1,2,3,4-tetrahydro-8-quinolinesulphonyl)-L-arginyl]-2-piperidine Carboxylic Acid (MQPA) to Human α-Thrombin. *Eur. J. Biochem*. **1990**, *193*, 175−182. (c) Brandstetter, H.; Turk, D.; Höffken, H. W.; Grosse, D.; Stürzebecher, J.; Martin, P. D.; Edwards, B. F. P.; Bode, W. Refined 2.3 Å X-ray Crystal Structure of Bovine Thrombin Complexes Formed with the Benzamidine and Arginine-based Thrombin Inhibitors NAPAP, 4-TAPAP and MQPA. *J. Mol. Biol*. **1992**, *226*, 1085−1099. (d) Banner, D. W.; Hadváry, P. Crystallographic Analysis at 3.0 Å Resolution of the Binding to Human Thrombin of Four Active Site-directed Inhibitors. *J. Biol. Chem*. **1991**, *266*, 20085−20093.

(8) Misra, R. N.; Kelly, Y. F.; Brown, B. R.; Roberts, D. G. M.; Chong, S.; Seiler, S. M. Argatroban Analogues: Synthesis, Thrombin Inhibitory Activity and Cell Permeability of Aminoheterocyclic Guanidine Surrogates. *Bioorg. Med. Chem. Lett.* **1994**, *4*, 2165−2170.

(9) Jendralla, H.; Seuring, B.; Herchen, J.; Kulitzscher, B.; Wunner, J. Efficient Kg-Scale Synthesis of Thrombin Inhibitor CRC 220. *Tetrahedron* **1995**, *51*, 12047−12068.

(10) Hilpert, K.; Ackermann, J.; Banner, D. W.; Gast, A.; Gubernator, K.; Hadváry, P.; Labler, L.; Müller, K.; Schmid, G.; Tschopp, T. B.; van der Waterbeemd, H. Design and Synthesis of Potent and Highly Selective Thrombin Inhibitors. *J. Med. Chem*. **1994**, *37*, 3889−3901.

(11) (a) Tucker, T. J.; Lumma, W. C.; Mulichak, A. M.; Chen, Z.; Naylor-Olson, A. M.; Lewis, S. D.; Lucas, R.; Freidinger, R. M.; Kuo, L. C. Design of Highly Potent Noncovalent Thrombin Inhibitors that Utilize a Novel Lipophilic Binding Pocket in the Thrombin Active Site. *J. Med. Chem*. **1997**, *40*, 830−832. (b) Tucker, T. J.; Lumma, W. C.; Lewis, S. D.; Gardell, S. J.; Lucas, B. J.; Baskin, E. P.; Woltmann, R.; Lynch, J. J.; Lyle, E. A.; Appleby, S. D.; Chen, I.; Dancheck, K. B.; Vacca, J. P. Potent Noncovalent Thrombin Inhibitors that Utilize the Unique Amino Acid D-Dicyclohexylalanine in the P3 Position. Implications on Oral Bioavailability and Antithrombotic Efficacy. *J. Med. Chem*. **1997**, *40*, 1565−1569.

(12) (a) Préville, P.; He, J. X.; Tarazi, M.; Siddiqui, M. A.; Cody, W. L.; Doherty, A. M. An Efficient Preparation of the Potent and Selective Pseudopeptide Thrombin Inhibitor, Inogatran. *Bioorg. Med. Chem. Lett.* **1997**, *7*, 1563−1566. (b) Teger-Nilsson, A.-C.; Bylund, R.; Gustafsson, D.; Gyzander, E.; Eriksson, U. In Vitro Effects of Inogatran, a Selective Low Molecular Weight Thrombin Inhibitor. *Thromb. Res.* **1997**, *85*, 133−145.

(13) (a) Obst, U.; Gramlich, V.; Diederich, F.; Weber, L.; Banner, D. W. Design of Novel Nonpeptidic Thrombin Inhibitors and Structure of a Thrombin-Inhibitor Complex. *Angew. Chem., Int. Ed. Engl.* **1995**, *34*, 1739−1742. (b) Obst, U.; Banner, D. W.; Weber, L.; Diederich, F. Molecular Recognition at the Thrombin Active Site: Structure-based Design and Synthesis of Potent and Selective Thrombin Inhibitors and the X-ray Crystal Structure of Two Thrombin-Inhibitor Complexes. *Chem. Biol*. **1997**, *4*, 287−295.

(14) Böhm, H.-J.; Klebe, G. What Can we Learn from Molecular Recognition in Protein−Ligand Complexes for the Design of New Drugs? *Angew. Chem., Intl. Ed. Engl.* **1996**, *35*, 2588−2614 and references therein.

(15) (a) Stewart, D. E.; Sarkar, A.; Wampler, J. E. Occurrence and Role of Cis Peptide Bonds in Protein Structures. *J. Mol. Biol.* **1990**, *214*, 253−260. (b) Eberhardt, E. S.; Loh, S. N.; Raines, R. T. Thermodynamic Origin of Prolyl Peptide Bond Isomers. *Tetrahedron Lett.* **1993**, *34*, 3055−3056.

(16) (a) Nagai, U.; Sato, K. Synthesis of a Bicyclic Dipeptide with the Shape of a β-Turn. *Pept. Chem*. **1984**, 207−210. (b) Nagai, U.; Sato, K. Synthesis of a Bicyclic Dipeptide with the Shape of a β-Turn Central Part. *Tetrahedron Lett.* **1985**, *26*, 647−650. (c) Nagai, U.; Sato, K.; Nakamura, R.; Kato, R. Bicyclic Turned Dipeptide (BTD) as a β-Turn Mimetic; its Design, Synthesis and Incorporation into Bioactive Peptides. *Tetrahedron* **1993**, *49*, 3577−3592.

(17) (a) Sato, K.; Nagai, U. Synthesis and Antibiotic Activity of a Gramicidin S Analogue Containing Bicyclic β-Turn Dipeptides. *J. Chem. Soc., Perkin Trans. 1* **1986**, 1231−1234. (b) Bach, A. C., II; Markwalder, J. A.; Ripka, W. C. Synthesis and NMR Conformational Analysis of a β-Turn Mimic Incorporated into Gramicidin S. *Int. J. Pept. Protein Res.* **1991**, *38*, 314−323. (c) Sato, K.; Hotta, M.; Dong, M.-H.; Hu, H.-Y.; Taulene, J. P.; Goodman, M.; Nagai, U.; Ling, N. Solid-Phase Synthesis of Human Growth Hormone-Releasing Factor Analogues Containing a Bicyclic β-Turn Dipeptide. *Int. J. Pept. Protein Res*. **1991**, *38*, 340−345. (d) Etzkorn, F. A.; Guo, T.; Lipton, M. A.; Goldberg, S. D.; Bartlett, P. A. Cyclic Hexapeptides and Chimeric Peptides as Mimics of Tendamistat. *J. Am. Chem. Soc*. **1994**, *116*, 10412−10425. (e) Rishton, G. M.; Harn, N. K.; Cripps, S. J.; Chiang, S.-L.; Mikos, C.; Cardarelli, P.; Lobl, T. J.; Gorcsan, F.; Moscinski, M.; Delaet, N. G. J.; Walker, S. M. A β-Turn Mimic and a Thiomethylene Dipeptide Surrogate Employed in the Study of Cyclic Peptide RGD and RCD Cell-Adhesion Inhibitors. *Lett. Pept. Sci.* **1996**, *3*, 37−44. (f) Haubner, R.; Schmitt, W.; Hölzemann, G.; Goodman, S. L.; Jonczyk, A.; Kessler, H. Cyclic RGD Peptides Containing β-Turn Mimetics. *J. Am. Chem. Soc.* **1996**, *118*, 7881−7891. (g) Doyle, P. M.; Harris, J. C.; Moody, C. M.; Sadler, P. J.; Martin, S.; Thornton, J. M.; Uppenbrink, J.; Viles, J. H. Solution Structure of a Biologically Active LDV Peptide Analogue Containing a Type II′ β-Turn Mimetic. *Int. J. Pept. Protein Res.* **1996**, *47*, 427−436. (h) Alberg, D. G.; Schreiber, S. L. Structure-Based Design of a Cyclophilin-Calcineurin Bridging Ligand. *Science* **1993**, *262*, 248−250.

(18) (a) Subasinghe, N. L.; Bontems, R. J.; McIntee, E.; Mishra, R. K.; Johnson, R. L. Bicyclic Thiazolidine Lactam Peptidomimetics of the Dopamine Receptor Modulating Peptide Pro-Leu-Gly-NH_2. *J. Med. Chem*. **1993**, *36*, 2356−2361. (b) Tamura, S. Y.; Goldman, E. A.; Brunck, T. K.; Ripka, W. C.; Semple, J. E. Rational Design, Synthesis, and Serine Protease Inhibitory Activity of a Novel P_1-Argininal Derivative Featuring a Conformationally

Constrained P_2-P_3 Bicyclic Lactam Moiety. *Bioorg. Med. Chem. Lett.* **1997**, *7*, 331−336. (c) Dolle, R. E.; Prasad, C. V. C.; Prouty, C. P.; Salvino, J. M.; Awad, M. M. A.; Schmidt, S. J.; Hoyer, D.; Ross, T. M.; Graybill, T. L.; Speier, G. J.; Uhl, J.; Miller, B. E.; Helaszek, C. T.; Ator, M. A. Pyridazinodiazepines as a High-Affinity, P_2-P_3 Peptidomimetic Class of Interleukin-1β-Converting Enzyme Inhibitor. *J. Med. Chem.* **1997**, *40*, 1941−1946.

(19) Osano, Y. T.; Nagai, U.; Matsuzaki, T. Crystal Structure of a β-Turn Model Dipeptide, (3*S*,6*S*, 9*R*)-2-Oxo-3-*tert*-butyloxycarboxylamino-7-thia-1-aza-bicyclo-[4.3.0]nonane-9-carboxylic Acid. *Anal. Sci.* **1989**, *5*, 625−626. The data of the X-ray structure of *S*-BTD are found in the Cambridge Structural Databank (Code SEYZUR).

(20) For the original procedure, see ref 16. A second approach was published by Bartlett et al., see ref 17d. Very recently, the Fmoc-protected *S*-BTD became commercially available from Neosystem.

(21) The ROESY spectrum of the major diastereoisomer **4a** showed a NOE effect between H−C_{2b} and H−C_9. On the other hand, the ROESY spectrum of **4b** indicated NOE effects between H−C_{2a} and H−C_9 as well as between H−C_9 and H−C_{7a}.

(22) Prepared according to Bergeron, R. J.; McMarris, J. S. Total Synthesis of (±)15-Deoxyspergualin. *J. Org. Chem.* **1987**, *52*, 1700−1703.

(23) Compound **18** is unstable and cyclizes to **18a** even at low temperatures:

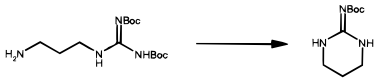

18 **18a**

(24) The protons H−C_2, H-C_3, H-C_6, H-C_7, H-C_8, and H−C_9 have been assigned using 2D-COSY and 2D-ROESY spectra in benzene. The relative stereochemistry between H−C_9 and H−C_3 of the major diastereoisomer has been determined to be trans by NOE measurements in DMSO. The stereochemistry has been confirmed by X-ray crystallography of the ligand **15** bound to thrombin.

(25) The programs CHARMM 23 and Quanta 4.0 were developed by MSI: Molecular Simulation Inc., San Diego, CA 92121-3752.

(26) Fenton, J. W., II; Fasco, M. J.; Stackrow, A. B.; Aronson, D. L.; Young, A. M.; Finlayson, J. S. Human Thrombins: Production, Evaluation, and Properties of α-Thrombin. *J. Biol. Chem.* **1977**, *252*, 3587−3598.

(27) Skrzypczak-Jankun, E.; Carperos, V. E.; Ravichandran, K. G.; Tulinsky, A.; Westbrook, M.; Maraganore, J. M. Structure of the Hirugen and Hirulog 1 Complexes of α-Thrombin. *J. Mol. Biol.* **1991**, *221*, 1379−1393.

(28) Messerschmidt, A.; Pflugrath, J. W. Crystal Orientation and X-ray Pattern Prediction Routines for Area Detector Diffractometer Systems in Macromolecular Crystallography. *Appl. Crystallogr.* **1987**, *20*, 306−315.

(29) Jones, T. A.; Zou, J.-Y.; Cowan, S. W.; Kjeldgraad, M. Improved Methods for Building Protein Models in Electron Density Maps and the Location of Errors in these Models. *Acta Crystallogr.* **1991**, *A47*, 110−119.

(30) Brünger, A. T. *X-PLOR Manual 3.1*; Yale University: New Haven, CT, 1992.

(31) Engh, R. A.; Huber, R. Accurate Bond and Angle Parameters for X-ray Protein Structure Refinement. *Acta Crystallogr.* **1991**, *A47*, 392−400.

(32) Stone, S. R.; Hofsteenge, J. Kinetics of the Inhibition of Thrombin by Hirudin. *Biochemistry* **1986**, *25*, 4622−4628.

(33) Dixon, M. The Determination of Enzyme Inhibition Constants. *Biochem. J.* **1953**, *55*, 170−171.

JM981013E